الجمهـــوريـــــة الجزائـــريـــــة الديمقـــراطيـــة الشـعبيـــة
République Algérienne Démocratique et Populaire
وزارة التـــعلـــيـــــم العـــــالـــــي والبـــحـــــث العـلمـــي
Ministère de l'Enseignement Supérieure et de la Recherche Scientifique
جامعة وهران 2 محمد بن أ حمد
Université d'Oran 2 Mohamed Ben Ahmed
معهد الصيانة و الأمن الصناعي
Institut de Maintenance et de Sécurité Industrielle

Département : Maintenance en Électromécanique

MÉMOIRE

Pour l'obtention du diplôme de Master

Filière : Électromécanique
Spécialité : Maintenance Industrielle et Électromécanique

Thème

Analysing the Thermal Power Output of Solar Collectors across Various Geographical Regions

Présenté et soutenu publiquement par :

WERIKHE Gilbert et MULYOWA David

Devant le jury composé de :

Nom et Prénom	Grade	Établissement	Qualité
HAMAMI Zineb	MCA	Université d'Oran 2	**Présidente**
DARRAMDANE Mohamed Zouhir	MCB	Université d'Oran 2	**Encadrant**
ABDI Ghezail	MCA	Université d'Oran 2	**Examinatrice**

Année 2024/2025

الجمهـوريـــة الجزائـريـــة الديمقـراطيـــة الشـعبيـــة
Peoples Democratic Republic of Algeria
وزارة التـــعلـــيـــم العـــالـــي والبـحـــث العـلمـــي
Ministry of Higher Education and Scientific Research
محمد بن أ حمد 2جامعة وهران
University of Oran 2 Mohamed Ben Ahmed
معهد السلامة الصناعية والصيانة
Institute of Industrial Safety and Maintenance

Department: Electromechanical Engineering and Maintenance

MASTER'S DISSERTATION

For obtaining a Master's Degree

Field: Electromechanical Engineering
Specialty: Industrial Maintenance and Electromechanics

Theme

Analysing the Thermal Power Output of Solar Collectors across Various Geographical Regions

Prepared and publicly defended by:

WERIKHE Gilbert and MULYOWA David

Infront of the Jury composed of:

Name	Rank	Institution	Position
HAMAMI Zineb	MCA	University of Oran 2	**President**
DARRAMDANE Mohamed Zouhir	MCB	University of Oran 2	**Supervisor**
ABDI Ghezail	MCA	University of Oran 2	**Examiner**

Academic Year 2024/2025

Acknowledgment.

We thank Almighty Allah for granting us the health, faith, and will to begin and complete this dissertation.

First of all, this work would not be substantial without the help and guidance of our supervisor, teacher and mentor Mr. Dar Ramdane Mohamed Zouhir in the department of Electromechanical Engineering, University of Oran 2 Mohamed Ben Ahmed**.** We thank him for the quality of his exceptional supervision, his patience, his rigor, and his availability during our preparation of this dissertation. Our thanks go to the president and the Juries for reviewing and contributing their interest to this work.

We also thank all our Professors for their generosity and the great patience they demonstrated despite their academic and professional responsibilities.

Dedication.

We dedicate our thesis to our families. A special feeling of gratitude goes to our beloved parents, whose words of encouragement and tenacity resonate in our ears.

We dedicate this thesis to our many friends who supported us throughout the process. We will always appreciate everything they did and their presence for us, to mention but a few; Tomusange Rodney, Touil Lakhdar, Sekkiou Sofiane El Hadj, Djafri Selman Ali and Otmani Nouba El Hachemi.

Table Of Contents.

GENERAL INTRODUCTION.....14

CHAPTER 1: LITERATURE REVIEW. 1

1.1 INTRODUCTION. 1
1.2 RECENT WORKS. 2
1.3 CONCLUSION. 3

CHAPTER 2: DESCRIPTION AND OPERATING PRINCIPLE OF THERMAL SOLAR COLLECTORS. 4

2.1 INTRODUCTION. 4
2.2 TYPES OF COLLECTORS: 4
2.2.1 NON-CONCENTRATING SOLAR COLLECTORS: 5
2.3 OPERATING PRINCIPLE: 9
2.3.1 CONCENTRATING SOLAR COLLECTORS: 10
2.4 APPLICATIONS OF SOLAR COLLECTORS: 12
2.5 CONCLUSION. 13

CHAPTER 3: MATHEMATICAL MODEL OF SOLAR PARAMETERS. 14

3.1 INTRODUCTION. 14
3.2 GENERAL INFORMATION ABOUT THE SOLAR PARAMETERS. 15
3.2.1 SUN -EARTH ANGLES (GEOMETRICAL PARAMETERS). 15
3.3 SOLAR TIME AND DURATION OF THE DAY. 20
3.3.1 DURATION OF THE DAY. 20
3.3.2 SOLAR TIME. 20
3.4 SOLAR RADIATION. 22
3.4.1 BEAM RADIATION (I_B): 23
3.4.2 DIFFUSE RADIATION (I_D): 23
3.4.3 THE TOTAL RADIATION (I): 23
3.5 IRRADIATION (RADIANT EXPOSURE): 23
3.6 SOLAR RADIATION INCIDENT ON A HORIZONTAL SURFACE. 24
3.6.1 EXTRATERRESTRIAL REGION. 24
3.6.2 HOURLY IRRADIATION (RADIATION RECEIVED IN HOURLY TIME INTERVALS). 25
3.6.3 DAILY EXTRATERRESTRIAL IRRADIATION (H_o): 25
3.6.4 THE MONTHLY AVERAGE DAILY EXTRATERRESTRIAL RADIATION ($\overline{Ho}$): 25
3.6.5 TERRESTRIAL REGION. 26
3.7 EVALUATION OF THE PARAMETERS USED FOR SOLAR RADIATION. 27
3.7.1 THE MONTHLY AVERAGE OF DAILY TOTAL RADIATION ($\overline{H}$) IN J/M^2 ON A HORIZONTAL SURFACE. 27
3.7.2 ESTIMATION OF BEAM AND DIFFUSE COMPONENTS OF DAILY SOLAR RADIATION. 27
3.7.3 MONTHLY AVERAGE CLEARNESS INDEX $\overline{KT}$ 28
3.7.4 ESTIMATION OF THE MONTHLY AVERAGE OF DAILY DIFFUSE SOLAR RADIATION ON A HORIZONTAL SURFACE. 28
3.7.5 ESTIMATION OF THE MONTHLY AVERAGE HOURLY DIRECT SOLAR RADIATION. 29

3.7.6 DIFFUSE HOURLY SOLAR RADIATION IN MONTHLY AVERAGE. 29
3.7.7 DIRECT HOURLY SOLAR RADIATION IN MONTHLY AVERAGE. 29
3.8 ESTIMATION OF SOLAR RADIATION ON AN INCLINED/TILTED SURFACE. 29
3.8.1 CONVERSION FACTORS. 29
3.8.2 CONVERSION FACTOR FOR BEAM SOLAR RADIATION. 30
3.8.3 CONVERSION FACTOR FOR DIFFUSE SOLAR RADIATION. 30
3.8.4 CONVERSION FACTOR FOR REFLECTED SOLAR RADIATION. 30
3.8.5 CONVERSION FACTOR OF HOURLY TOTAL SOLAR RADIATION ON AN INCLINED/TILTED SURFACE. 31
3.8.6 CONVERSION FACTOR FOR DAILY TOTAL SOLAR RADIATION ON AN INCLINED SURFACE. 31
3.8.7 CONVERSION FACTOR FOR MONTHLY AVERAGE DAILY TOTAL SOLAR RADIATION ON AN INCLINED SURFACE. 31
3.9 TOTAL SOLAR RADIATION ON AN INCLINED/TILTED SURFACE. 31
3.9.1 MONTHLY AVERAGE DAILY SOLAR RADIATION *HT* ON INCLINED SURFACE. 32

CHAPTER 4: ALGORITHM AND COMPUTATIONAL PROGRAM USING MATLAB. 33

4.1 THE FLOWCHART OF THE CALCULATION PROGRAM. 36
4.2 CONCLUSION. 37

CHAPTER 5: RESULTS AND DISCUSSIONS. 38

5.1 VALIDATION OF THE MODEL. 38
5.1.1 ENTEBBE, KAMPALA (0.06°N, 32.44°E). 38
5.1.2 STOCKHOLM, SWEDEN (59.33°N, 18.06°E). 39
5.1.3 BLOEMFONTEIN, SOUTH AFRICA (29.10°S, 26.20°E). 40
5.1.4 COMPARISON OF SOLAR IRRADIANCE. 42
5.1.5 COMPARISON OF THE OUTLET FLUID TEMPERATURE. 44
5.1.6 COMPARISON OF THE THERMAL POWER OUTPUT. 46
5.1.7 SOLAR COLLECTOR EFFICIENCY 48
5.1.8 COMPARISON BETWEEN AVERAGE MONTHLY THERMAL AND PV POWER OUTPUT FOR THE MONTHS OF JANUARY, JULY AND OCTOBER. 49
5.1.9 AVERAGE YEARLY THERMAL POWER OUTPUT OF SOLAR COLLECTORS. 51
5.1.10 COMPARISON BETWEEN AVERAGE YEARLY THERMAL AND PV POWER OUTPUT. 52

GENERAL CONCLUSION. 53

REFERENCES. 54

LIST OF FIGURES.

FIGURE 2-1: EVACUATED TUBE COLLECTOR 5
FIGURE 2-2: THERMOSIPHON FLAT PLATE COLLECTOR 6
FIGURE 2-3: FLAT PLATE COLLECTOR 6
FIGURE 2-4: PARTS OF A FLAT PLATE COLLECTOR 7
FIGURE 2-5: PARABOLIC TROUGH COLLECTOR 10
FIGURE 2-6: PARABOLIC DISH COLLECTOR 11
FIGURE 2-7: HELIOSTAT FIELD COLLECTOR 11
FIGURE 2-8: LINEAR FRESNEL REFLECTOR 12
FIGURE 2-9: COMPACT LINEAR FRESNEL REFLECTOR 12
FIGURE 3-1: VIEW OF DIFFERENT SUN EARTH ANGLES 15
FIGURE 3-2: VIEW OF DIFFERENT SUN EARTH ANGLES 15
FIGURE 3-3: HOUR ANGLE FOR A POINT. 17
FIGURE 3-4: VIEW OF VARIOUS SUN EARTH ANGLES ON AN INCLINED SURFACE 18
FIGURE 3-5: DIRECT, REFLECTED AND BEAM RADIATIONS 23
FIGURE 5-1 COMPARISON BETWEEN ANALYTICAL MODEL AND CALCULATED DATA (PVGIS) FOR ENTEBBE ON 20TH MAY 38
FIGURE 5-2 COMPARISON BETWEEN ANALYTICAL MODEL AND CALCULATED DATA (PVGIS) FOR STOCKHOLM ON 20TH MAY 39
FIGURE 5-3 COMPARISON BETWEEN ANALYTICAL MODEL AND CALCULATED DATA (PVGIS) FOR BLOEMFONTEIN ON 20TH MAY 40
FIGURE 5-4 RELATIVE ERROR OF MODEL FOR THE THREE CITIES ON 20TH MAY 41
FIGURE 5-5: SOLAR IRRADIANCE FOR JANUARY FOR ALL CITIES 42
FIGURE 5-6: SOLAR IRRADIANCE FOR JULY FOR ALL CITIES 42
FIGURE 5-7: SOLAR IRRADIANCE FOR OCTOBER FOR ALL CITIES 43
FIGURE 5-8: OUTLET FLUID TEMPERATURE FOR JANUARY FOR ALL CITIES 44
FIGURE 5-9: OUTLET FLUID TEMPERATURE FOR JULY FOR ALL CITIES 44
FIGURE 5-10: OUTLET FLUID TEMPERATURE FOR OCTOBER FOR ALL CITIES 45
FIGURE 5-11 THERMAL POWER OUTPUT OF JANUARY FOR ALL 4 CITIES 45
FIGURE 5-12 THERMAL POWER OUTPUT OF JULY FOR ALL CITIES 46
FIGURE 5-13 THERMAL POWER OUTPUT OF OCTOBER FOR ALL CITIES 47
FIGURE 5-14 COMPARISON OF THERMAL COLLECTOR EFFICIENCY BY CITY 48
FIGURE 5-15 THERMAL AND PV AVERAGE MONTHLY POWER OUTPUT OF JANUARY FOR ALL CITIES 49
FIGURE 5-16 THERMAL AND PV AVERAGE MONTHLY POWER OUTPUT OF JULY FOR ALL CITIES 49
FIGURE 5-17 THERMAL AND PV AVERAGE MONTHLY POWER OUTPUT OF OCTOBER FOR ALL CITIES 50
FIGURE 5-18: AVERAGE YEARLY THERMAL POWER OUTPUT FOR ALL CITIES 51
FIGURE 5-19: COMPARISON OF AVERAGE YEARLY POWER OUTPUT FOR ALL 4 CITIES 52

List of Equations.

(3-1) 16
(3-2) 17
(3-3) 17
(3-4) 18
(3-5) 19
(3-6) 19
(3-7) 19
(3-9) 19
(3-8) 19
(3-10) ---- 20
(3-11) ---- 20
(3-12) ---- 20
(3-13) ---- 20
(3-14) ---- 20
(3-15) ---- 21
(3-16) ---- 21
(3-17) ---- 21
(3-18) ---- 22
(3-19) ---- 22
(3-20) ---- 23
(3-21) ---- 24
(3-22) ---- 24
(3-23) ---- 25
(3-24) ---- 25
(3-25) ---- 26
(3-26) ---- 26
(3-29) ---- 26
(3-28) ---- 26
(3-27) ---- 26
(3-30) ---- 26
(3-31) ---- 26
(3-32) ---- 27
(3-33) ---- 27
(3-34) ---- 27
(3-35) ---- 27
(3-36) ---- 28
(3-37) ---- 28
(3-38) ---- 28
(3-39) ---- 29
(3-40) ---- 29
(3-41) ---- 29
(3-43) ---- 29
(3-42) ---- 29
(3-44) ---- 29
(3-45) ---- 30
(3-46) ---- 30
(3-47) ---- 30
(3-48) ---- 30
(3-49) ---- 31
(3-50) ---- 31

(3-51) ---------- 31
(3-52) ---------- 31
(3-53) ---------- 31
(3-54) ---------- 31
(3-55) ---------- 31
(3-56) ---------- 32
(3-57) ---------- 32

List of Tables.

TABLE 3-1 VALUES JULIAN'S DAY BY MONTH. 21
TABLE 3-2 LATITUDE, LONGITUDE, AND ELEVATION FOR DIFFERENT PLACES IN THE WORLD. 22
TABLE 3-3 THE DAY TYPES OF EACH MONTH 25

Nomenclature

N	Number of daylight(sunshine) hours
n	Day of the year
I_N	Normal Solar radiation
I_{on}	Extraterrestrial radiation on the earth's surface
m	Air mass
T_R	Turbidity factor (cloudiness factor).
α	Lumped atmospheric parameter
ε	Integrated optical thickness of the terrestrial clear and dry atmosphere/ Rayleigh atmosphere.
h	Height of the sun.
I_{on}	Extraterrestrial radiation on the earth's surface
I'_{oh}	Hourly irradiation
I_b	Beam radiation
I_d	Diffuse radiation
I	Total radiation
I_{sc}	The radiant solar (energy) flux
I'_{oh}	Hourly irradiation
H_o	Daily irradiation [J/m^2]
I_h	hourly total solar radiation
ρ	Reflection coefficient (albédo)
I_b	Hourly direct (beam) solar radiation on a horizontal surface.
I_d	Hourly diffuse solar radiation on a horizontal surface.
R_t	Conversion factor for the hourly monthly average global radiation
R_r	Reflected solar radiation
$\overline{R}_b$	Conversion factor for average daily beam radiation
R_d	Conversion factor for diffuse radiation
$\frac{H_d}{H}$	Ratio of daily diffuse radiation to daily total solar radiation
K_T	Daily clearness index

Greek Symbols

Φ	latitude Angle
φ	Latitude of the place
δ	Declination Angle
η	Efficiency
β	Slope
ω	Hour Angle
ω_s	Hour angle at sunset
ω_1, ω_2.	Hourly angles corresponding to the two solar times
γ	Surface Azimuth
γ_s	Solar Azimuth
θ_z:	Zenith angle
θ_Z and θ_i	angles of incidence on the horizontal and inclined surfaces respectively

Abbreviations

ST	Solar Time
LT	Local standard Time
L_{Loc}	Longitude of the location
L_{ST}	Standard meridian for a local zone
ET	Equation of time
PVGIS	Photovoltaic Geographical Information System

الملخص

تبحث هذه المذكرة في إنتاج الطاقة الحرارية لمجمعات الطاقة الشمسية عبر مناطق جغرافية مختلفة، وتحليل كيفية تأثير التغيرات في الإشعاع الشمسي والمناخ على أداء النظام. تركز الدراسة على أربع مدن متميزة هي عنتيبي (أوغندا)، وستوكهولم (السويد)، وغرداية (الجزائر)، وبلومفونتين (جنوب إفريقيا) التي تمثل المناخات الاستوائية والشمالية والجافّة والجنوبية على التوالي. تم تطوير نموذج تحليلي قائم على ماتلاب (Matlab)، يدمج لمُعاملات الشمسية. يتم تقدير الإشعاع الأفقي الكلي اليومي باستخدام نموذج أنجستروم بريسكوت وتوزيعه على قيم كل ساعة باستخدام طريقة كولاريس-بيريرا ورابل، ثم يتم اسقاط الإشعاع بعد ذلك على سطح مُجمِّع مائل لإدخاله كبيانات إلى النموذج الحراري لمُجمِّع الألواح المُسطحة. م التحقق من صحة النتائج التحليلية مقابل بيانات من نظام المعلومات الجغرافية الكهروضوئية الذي يوفر بيانات سنوية عن الإشعاع الشمسي لمدن مختارة. تم تقدير الناتج الحراري للمجمع ذي اللوحة المسطحة باستخدام برنامج محاكات معد مسبقا، مع مراعاة الظروف المحيطة المتغيرة ومعدل تدفق كتلة ثابت قدره 0.002 كجم/ثانية. ت. تكشف النتائج أن الأداء الحراري يختلف بشكل كبير حسب الموقع الجغرافي والتوافر الشمسي الموسمي. لوحظ ارتفاع الناتج في المواقع ذات الإشعاع العالي مثل غرداية وبلومفونتين، بينما لوحظ انخفاض الأداء في ستوكهولم بسبب انخفاض الإشعاع في فصل الشتاء. تشير مقارنة الطاقة الحرارية والطاقة الكهروضوئية إلى أن استخدام نظام الطاقة الشمسية الحرارية ضئيل فوق وتحت خطوط العرض 30 درجة و-30 درجة على التوالي، حيث تُعدّ الطاقة الكهروضوئية في تلك المناطق الخيار الأمثل.

Abstract

This memoir investigates the thermal energy production of solar collectors across different geographic regions, analyzing how variations in solar radiation and climate affect system performance. The study focuses on four distinct cities: Entebbe (Uganda), Stockholm (Sweden), Ghardaia (Algeria) and Bloemfontein (South Africa), representing tropical, boreal, arid and southern climates respectively. A Matlab-based analytical model was developed, integrating solar parameters. The daily global horizontal radiation is estimated using the Angstrom-Prescott model and distributed to hourly values using the Collares-Pereira-Rable method. The radiation is then projected onto a tilted collector surface to introduce it as an input data to the thermal model of the flat plat collector. The analytical results are validated against data from a photovoltaic geographic information system (GIS), which provides annual solar radiation data for selected cities. The thermal output of the flat-plate collector is estimated using an existing simulation program, taking into account variable ambient conditions and a constant mass flow rate of 0.002 kg/s. The results reveal that thermal performance varies significantly depending on geographic location and seasonal solar availability. Higher output is observed in high-irradiance locations such as Ghardaia and Bloemfontein, while lower performance is observed in Stockholm due to low winter irradiance. The comparison between the thermal and photovoltaic power indicate that the use of thermal solar system is insignificant in the areas above and below the latitude of 30° and -30° respectively where photovoltaic is the optimal choice.

General Introduction.

This dissertation focuses on analysing the thermal power output of solar collectors across different geographical locations. The study aims to understand how location-specific climatic conditions impact the efficiency and thermal performance of flat plate collectors. This is achieved by developing a comprehensive mathematical model and implementing it through a computational program in Matlab, this research provides a comparative analysis of solar collector performance in a few selected cities. The dissertation is structured around five chapters:

Chapter 1 reviews existing research on solar energy systems, with a particular focus on flat plate solar collectors. It discusses previous methodologies used for performance analysis and identifies key parameters affecting collector output.

Chapter 2 provides a detailed overview of the structure and working principles of flat plate solar collectors. It explains the energy conversion processes and the role of each component in the collector system.

Chapter 3 is where a mathematical model is developed by the help of existing working examples and scientific formulas to describe the thermal performance of the collector. The model incorporates solar radiation input, thermal losses, and fluid properties to calculate the useful energy gain.

Chapter 4 presents the computational approach used to analyse the collector's performance. It details the Matlab code and algorithm structure, explaining how input data is processed to generate performance metrics.

The final chapter 5 presents the Analytical results for various geographical locations. It commences with a validation of the developed model and includes a comparative analysis of the solar irradiance, thermal power output, outlet fluid temperature and averages. The results are discussed in relation to local climatic conditions, providing insights into optimal locations for solar thermal energy use.

Chapter 1: Literature Review.

1.1 Introduction.

Solar collector is a kind of heat exchanger where heat exchange takes place between a distant source and a heat transfer fluid flowing in the collector.

Solar radiation from sun hits the absorber plate of the collector and the thermal energy is then transferred to the fluid.

Based on their design, solar collectors can be classified as concentrating and non-concentrating type. Non-concentrating type can be further divided in flat plate collector and evacuated tube collectors.

Flat plate collectors are the most common type of collectors and the most primitive too. Work of Hottel and Woertz[1] and by Hottel and Whiller [2] in 1958 can be looked as a first work on solar flat plate collector. They had developed the collectors consisting of a black flat plate absorber, a transparent cover, heat transfer fluid and an insulating case. Tabor [3] in 1955, employed selective black surfaces to increase collector efficiency. His experiments on optical concentration revealed the ability of optical concentration to produce high pressure steam.

Many studies have been done after that to analyse and improve the thermal efficiency of the collector. Due to growing energy problems, solar energy is been looked at as source of infinite energy. Solar collectors have been greatly studied in this matter. Many of the new designs have been developed after 1990.

Various research works are being carried out over the world to improve the thermal performance of flat plate collectors. Polymers are used to build novel collectors so as to reduce the weight. Use of nanofluids makes the collectors compact by giving the same output as that of big collectors but in a comparatively smaller size. Absorber plates have undergone many modifications with the help of new and better techniques in manufacturing and material science [4].

Analysing the performance of collector is equally important as it helps to further develop and improve the design. In fact, development and analysis always go hand in hand. Experimental analysis of all the different collectors developed is not feasible. Hence analytical and numerical methods have been employed, to approximately analyse the behaviour of collector in different conditions.

The thermal performance of flat plate collectors and concentrated solar collectors varies significantly across different geographical regions due to variations in solar irradiance, climate conditions, and system design. Studies indicate that concentrated solar collectors, such as parabolic troughs and Fresnel reflectors, achieve higher thermal power outputs in regions with high direct normal irradiance (DNI), such as deserts (e.g., the Middle East, Atacama, and Sahara), where their optical concentration and tracking systems maximize energy capture [5].

In contrast, flat plate collectors demonstrate superior performance in temperate and cloudy climates (e.g., Northern Europe, Japan), where diffuse radiation dominates, and their ability to utilize scattered sunlight proves advantageous [6].

Geographical factors such as latitude, ambient temperature, and atmospheric conditions further influence collector efficiency. Research by Fernández-García et al. (2010) highlights that concentrated solar collectors suffer efficiency losses in high-wind or hazy environments, whereas flat plate collectors maintain more stable output due to their simpler design [7].

Additionally, seasonal variations impact concentrated solar collectors' performance more severely at higher latitudes, where lower sun angles reduce effective concentration[8]. The proposed work aims to predict the theoretical solar intensity as a function of temporal (during the year) and geographical location. These results will be introduced as input to an existing flat plate and concentrated solar software in order to compare and analyse the output solar thermal behaviors.

1.2 Recent works.

Recent studies have provided valuable insights into the comparative performance of flat plate collectors and concentrated solar collectors across various climatic regions. For instance, a 2020 study evaluated the performance of parabolic trough collectors and flat plate collectors in Tianjin, China, revealing that flat plate collectors were more suitable for hot water supply and heating, while parabolic trough solar collectors excelled in cooling applications due to their higher efficiency in direct solar irradiance conditions [9].

Another study conducted simulations using TRNSYS software to compare flat plate collectors and evacuated tube collectors in Naples, Stockholm, and Kabul. The findings indicated that evacuated tube collectors outperformed flat plate collectors in colder climates like Stockholm, owing to reduced thermal losses, whereas flat plate collectors showed better performance in warmer regions such as Naples [10].

In Turkey, research comparing available solar radiation for flat-plate and concentrating collectors highlighted that concentrated solar collectors are more effective in regions with high direct normal irradiance, while flat plate collectors are advantageous in areas with higher diffuse radiation [11].

Additionally, a techno-economic analysis of hybrid systems combining flat plate collectors and parabolic trough collectors demonstrated that such configurations could achieve higher solar fractions and lower levelized costs of heat, especially in industrial applications with varying radiation levels. These studies collectively underscore the importance of considering regional climatic conditions when selecting between flat plate collectors and concentrated solar collectors for optimal thermal performance [12].

1.3 Conclusion.

The thermal power output of flat plate and concentrated solar collectors is closely tied to the specific environmental conditions of different geographical regions.

Flat plate collectors are generally more suitable for areas with moderate to high levels of diffuse solar radiation, such as regions with frequent cloud cover or lower direct sunlight.

On the other hand, concentrated solar collectors perform best in locations with high direct normal irradiance, typically found in arid or semi-arid climates.

Research conducted across various locations demonstrates that no single collector type performs best everywhere; instead, the choice depends on factors like solar availability, temperature fluctuations, and local weather patterns.

Many recent studies also explore how technological advancements, such as improved materials, hybrid systems, and thermal storage, can enhance performance across different settings.

Overall, this highlights the importance of conducting region specific assessments when selecting solar thermal technologies to ensure optimal energy output and system efficiency.

Chapter 2: Description and Operating Principle of Thermal Solar Collectors.

2.1 Introduction.

Solar energy is a key renewable resource, widely utilized for thermal applications through solar collectors. Two primary types of solar thermal collectors are flat plate collectors and concentrating solar collectors, each designed for specific applications and efficiency requirements.

Flat plate solar collectors are commonly used for low- to medium-temperature applications such as domestic water heating and space heating, while concentrating solar collectors are employed in high-temperature applications, including power generation and industrial processes [13].

Flat plate collectors consist of a dark absorber plate that captures solar radiation and transfers the heat to a working fluid, typically water or air, flowing through tubes attached to the plate. These collectors are simple, cost-effective, and suitable for non-concentrated solar energy applications [14].

Conversely, concentrating solar collectors use optical components such as mirrors or lenses to focus sunlight onto a smaller receiver, increasing the temperature and efficiency of energy conversion. Common types of concentrating solar collectors include parabolic troughs, solar towers, and Fresnel reflectors, which achieve higher thermal efficiencies due to their ability to concentrate direct solar radiation [14].

This chapter examines the operating principles and theoretical analysis of these solar collectors. By understanding the theoretical foundation of flat plate and concentrating solar collectors, engineers and researchers can improve system designs, enhance efficiency, and expand the practical applications of solar thermal energy. The insights presented in this chapter contribute to the broader goal of sustainable energy development.

2.2 Types of Collectors:

A solar collector's main purpose is to absorb solar radiation of the sun and convert it into heat energy by transferring heat to the working fluid. There are mainly two types of solar collectors:

1. Non concentrating solar collectors
2. Concentrating solar collectors

2.2.1 Non-concentrating Solar Collectors:

Non-concentrating solar collectors are usually used for low temperature applications. These collectors consist of flat surface which absorbs heat from the sun. The efficiency of non-concentrating collectors is comparatively less but in terms of cost and maintenance these are much feasible. There are a few types non-concentrating solar collectors.[15][16] [17]

2.2.1.1 Evacuated Tube Collector:

Evacuated tube collector differs from the flat plate collector in construction and operation. Evacuated collectors are used in climates with high temperature or where the temperature is too high for flat plate collector to work efficiently. Evacuated tube collectors consist of a heat pipe inside a vacuum sealed tube. The heat pipe is made of copper for high heat absorbance. In these collectors, liquid-vapour phase change materials are used for high efficiency heat transfer.[18]

Another type of collector present consists of two concentric annealed glass tube with vacuum between the layers. The glass tubes are usually made of borosilicate glass. The inner tube works as the absorber of the solar radiation which is coated with selective absorber coating. The vacuum, by creating isolation between the tubes helps to reduce the heat losses by convection and conduction and hence increases the efficiency of the collector. It acts by the principle of a thermos flask. Evacuated tube collector can absorb both beam and diffused radiation.[15][16][19]

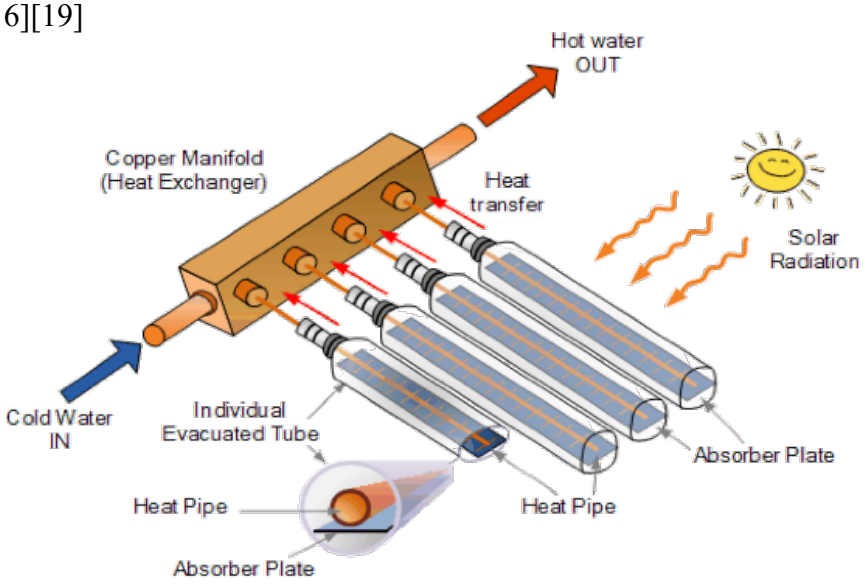


Figure 2-1: Evacuated Tube Collector

2.2.1.2 Thermosiphon collector:

Thermosiphon collectors are similar to flat plate collectors in working. They are used for heating water in a tank for domestic and household purposes. These collectors are set in the tank where water is to be heated and it heats the water to a temperature near 50°- 60°C.[19]

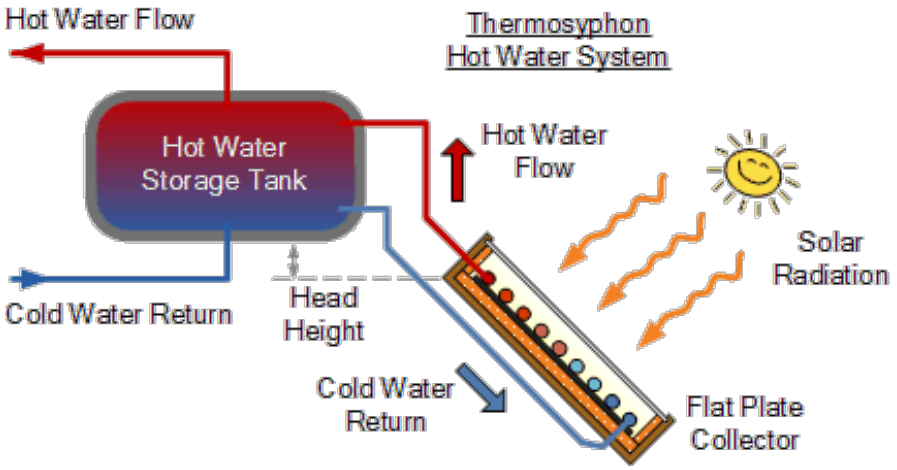


Figure 2-2: Thermosiphon flat plate collector

2.2.1.3 Flat Plate Solar Collector:

Flat plate solar collector is a very basic type of solar collector. It has a flat rectangular surface as an absorber. It is very efficient and convenient for temperatures up to 100°C.[17] These collectors are classified as liquid type and air type based on their heating application. A Flat plate collector is usually set up at the top of a building or a structure or in an open field and it uses both beam and diffused solar radiation for heating up. Several types of flat plate collectors have been designed since the 1900s by using different types of materials for improvement of performance as well as making it cheaper and more long-lasting.

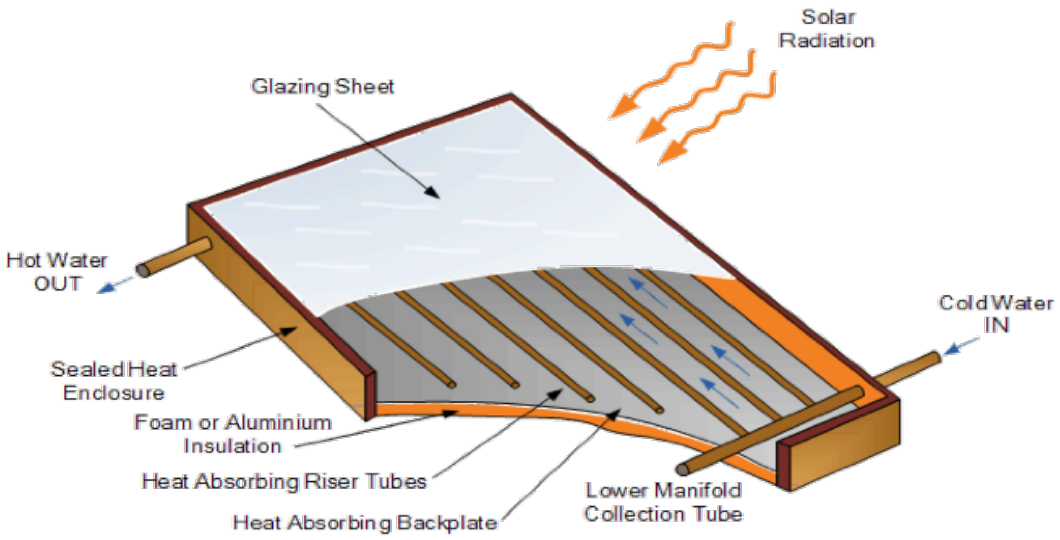


Figure 2-3: Flat plate collector

2.2.1.3.1 The structure and Construction of a Flat plate Solar collector:

A typical flat plate solar collector consists of a glazed absorber plate, tubes, thermal insulation, cover strip, insulated casing. Flat plate collectors are usually permanently fixed on a roof top or an open field and don't require any sun tracking system. The collectors are to be oriented directly towards the equator, facing south in the northern hemisphere and north in the southern. The optimum tilt angle of the collector must be equal to the latitude of the location with angle variations of 10–15° more or less depending on the application. A short description of the parts of a typical flat plate collector is given here.[15][18][19]

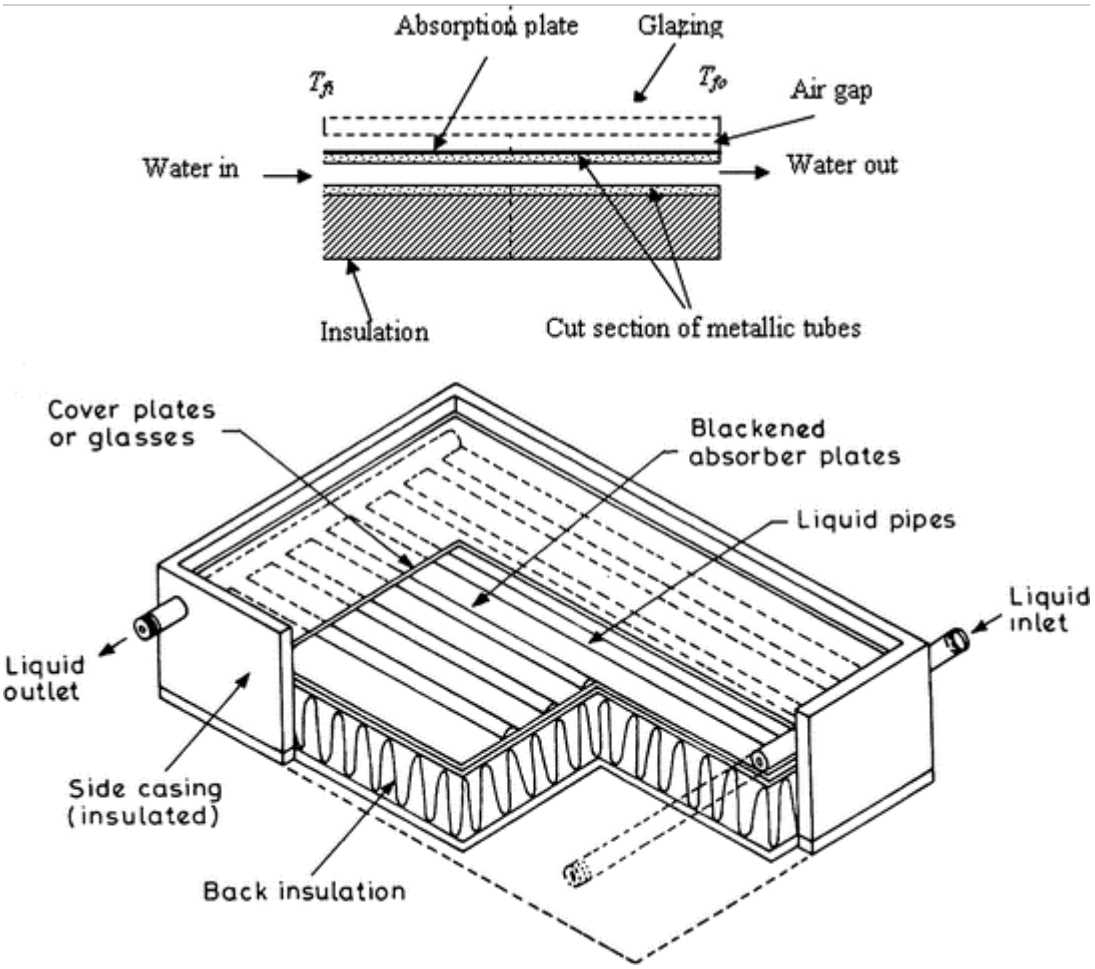


Figure 2-4: Parts of a Flat Plate Collector

a) Absorber Plate:

The absorber plate is a rectangular sheet made of high heat conducting material, especially copper or aluminium because of their high heat conductivity. It is usually painted in black and coated with absorptive material to get the maximum absorption of solar radiation.[17]

This thin layer is highly absorbent to shortwave solar radiation but comparatively translucent to long wave radiation. Another thin layer is provided below the coating with high reflectance to long wave radiation. The absorber plate absorbs the sun's heat energy and transfer that to the working fluid with minimum heat loss.[20][21][22]

b) Headers:

Tubes of large diameter are placed at the top and bottom of the absorber plate for the entrance and discharge of fluid. The header pipes are made of copper for maximum heat conduction from the absorber plate.[17] These header pipes are connected to the copper tubes by welding.[23]

c) Tubes:

Several tubes made of copper are placed on the absorber plate. The working fluid flows through the tubes where they are heated. The copper tubes are positioned parallel to each other on the absorber plate.[22]

The liquid tubes are connected at both ends by large diameter header tubes. These are soldered and brazed to the absorber plate so that smooth heat transfer takes place between them by getting maximum surface contact.[15][16][17]

d) Glazing:

Glazing refers to covering with glass or plastic having radiative properties. A flat plate collector has single, double or multiple layers of glazing above the blackened absorber plate. Low iron glass is mainly used for glazing having high transmissivity of short-wave radiation and low or zero transmissivity of long-wave radiation.[17]

The main purpose of glazing is to allow as much solar radiation as possible and create an insulation of the absorber plate with the environment by entrapping radiation to reduce convective losses as well as radiative losses. Transmission of short-wave radiation can also be increased by anti-reflective coating and surface texture. The glazing materials don't absorb heat like absorber plate.[15][16][21]

e) Insulation:

Insulation is provided to the sides and bottom of the flat plate collector to reduce heat loss. Different insulating materials like rubber, cotton, wool is used for this purpose. Insulating substances decrease heat loss from the absorber plate and help in heating the tubes as well as the plate.[15][21]

f) Casing:

A steel or wooden casing is used to hold the parts together. In the casing a layer of insulation is provided at the bottom. The absorber plate is placed after that copper tubes are incorporated in it. The sides are also insulated for the reduction of heat loss through convection.[17]

Finally, the glazing is done with glass to provide air gap between absorber and the atmosphere. All the parts are soldered, brazed or welded properly to get maximum surface contact and high heat transfer. Casing protects the parts from environmental influences like dust particles, rainfall, moisture.[16][21]

2.3 Operating Principle:

A solar collector works as a water heater and is based on the transformation of the absorbed solar radiation to thermal energy. In general, solar collector works by absorbing solar radiation which incidents on the collector plate passing through the glazed glass. The absorbed heat is then transferred to the working fluid flowing through the connected copper tubes with minimum heat loss. The heated fluid is then moved to the place of its use or to a storage tank for later use.[17]

A solar collector heating system is two types- active or direct and passive or indirect. Active or direct solar collector is basically an open-loop system. In this system, a differential temperature sensor is used to compare the temperature of the water to be heated. The heat collected by the collector is transferred to the working fluid which goes directly to the storage tank and then supplied to the household needs. A heat pump is used which draws cold water from the bottom of the storage tank and circulates it through the solar collector. As a result, the heated water is circulated through the tanks directly from the collector.[15][16][24]

Open loop system is of two types drain down system and the recirculating system. In the drain-down system a valve is used to allow the solar collector to fill with water when the collector reaches a certain temperature. In the recirculating system water is pumped through the collector when the temperature in the storage tank reaches a certain critical value.

Passive or indirect system is a closed-loop system. In this system, a heat transfer fluid called glycol is used to circulate through the solar collector. Glycol after absorbing radiant heat from the collector is passed to a heat exchanger where it heats the working fluid through heat transfer. Glycol works as anti-freezing substance and can operate efficiently at freezing temperature. The working fluid after being heated from the heat exchanger is transferred to a storage tank for after use.[25][26]

Thermo-siphon system is a kind of passive system which consists of an insulated storage tank set above the collectors. The heated fluid moves to the storage tank by convective process and stored there. In response, the cold fluid circulates to the collector and gets heated up. In this system, flow of fluid is slow. This system is simple and uses no energy and requires comparatively low maintenance.[27]

Air flat plate collectors work with the same principle but are used for conditioning of household or commercial premises. They work by natural or forced convection depending on absorbed heat. In air heating systems, A boiler is used to heat the air before using for space heating. A blower or fan may also be used for forced flow of air in other applications.[28]

2.3.1 Concentrating Solar Collectors:

Concentrating solar collectors are usually used for high temperature applications more than 100°C. Concentrating collectors may be reflectors or refractors. Wide variations are present in their design-parabolic, circular, cylindrical, convex or concave etc.

Concentrating collectors focus sunlight using lens and mirrors. The collectors maybe glazed or unglazed depending on the requirement. There have both sun tracking system as the sun's position changes with time as well as non-tracking system. They are also divided in two types as line focusing and point focusing. A few types of concentrating collectors are present.[15][29][19]

2.3.1.1 Parabolic Trough Collector:

Parabolic trough collector is a line focusing type of solar collector where the radiation of the sun is focused along the focus of the parabolic trough. Parabolic trough collectors are made by bending a reflective sheet into parabolic shape. An absorber pipe covered with glass tube to protect it from dust and moisture which reduces reflectivity is placed along the focal line and working fluid usually water flows through it. The sun rays are reflected and falls on the absorber tube which heats the working fluid.[17]

The absorber or receiver tube is coated with material of high solar radiation absorptance and the glass layer helps in reduction of thermal losses by convection and radiation. By the use of one-axis tracking device, which tracks the sun position in one direction only, either east-west or north-south, the position and focus of the solar radiation changes with the elevation of the sun. The collector pipe or the trough are rotated along the axis of the absorber pipe continuously. Temperature up to 400°C can be obtained using this collector. Parabolic trough collectors are the most advanced solar collector technologies and mainly used for solar thermal electricity generation.[27][16]

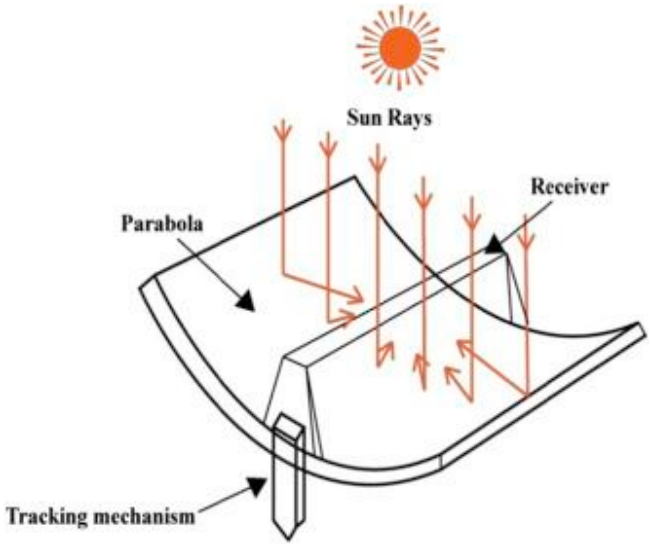


Figure 2-5: Parabolic Trough Collector

2.3.1.2 Parabolic Dish Collector:

It is a point focusing type of solar collector. The receiver is placed at the focus of the concentrator or dish. The sun's radiation is collected at the receiver.[30] It uses two axis sun tracking system. It is used for high temperature works above 1500°C. Working fluid circulates through the receiver. A Parabolic Dish collector is mainly used for small electricity generation using sunlight. It is the most efficient among all collectors.[15][29]

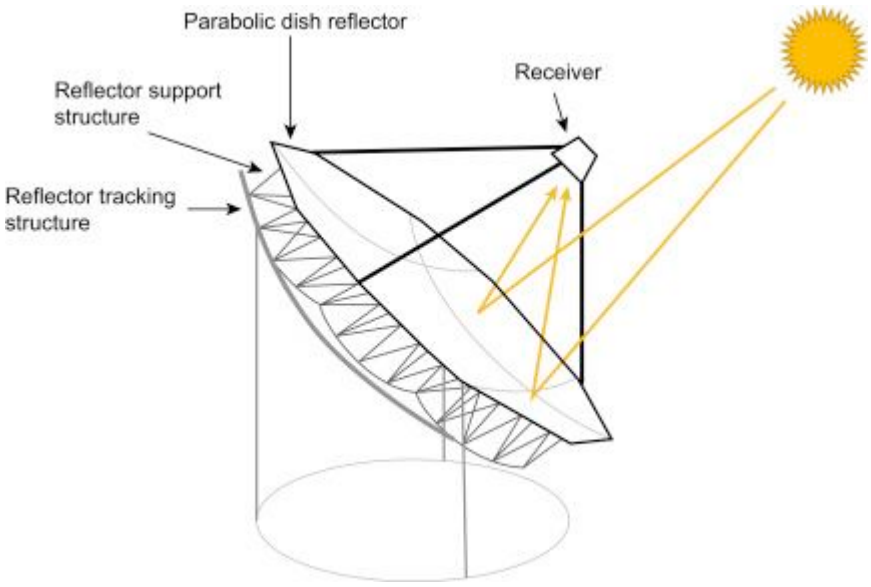


Figure 2-6: Parabolic Dish Collector

2.3.1.3 Heliostat Field Collector:

It consists of a number of flat mirrors called heliostats spread over a large region. Altazimuth mounts are used for setting up the mirrors. The heliostats focus the sun's radiation to a common tower usually 500m long.

The collector or receiver is placed in the central tower which consist of vertical tubes of flowing water. Up to 1500°C temperature is achievable using this collector. The heliostats are controlled by automated tracking device to change position with respect to the sun. Heliostat collectors are used for power generation using high temperature steam generated from heating the working fluid.[15][29]

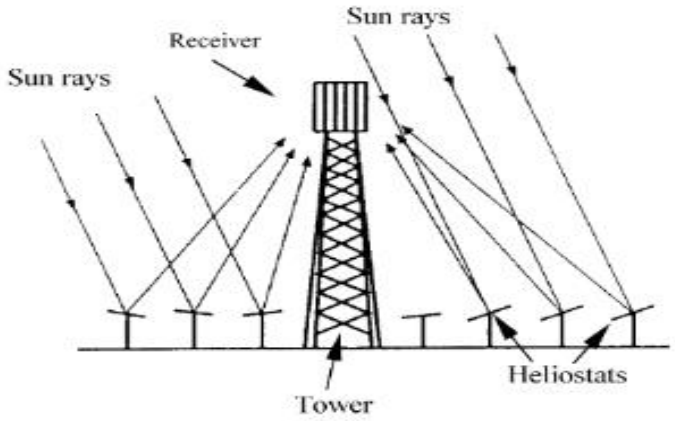


Figure 2-7: Héliostat Field Collector

2.3.1.4 Fresnel Lens Concentrating Collector:

In this collector Fresnel lens is used. Fresnel lens is flat on one side and provided with linear grooves on the other side. The grooves possess optical quality for which the behave like a common lens. The absorber tube is oriented in such a way that the radiation after refraction through the lens is focused at the tube.

Another type of collector is the linear Fresnel reflector which consists of a linear arrangement of flat or curved elastic mirrors focusing light on a receiver mounted on the top a linear tower.[15][29]

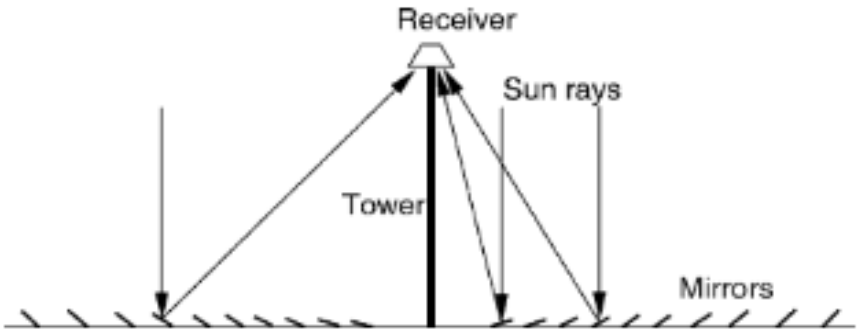


Figure 2-8: Linear Fresnel Reflector

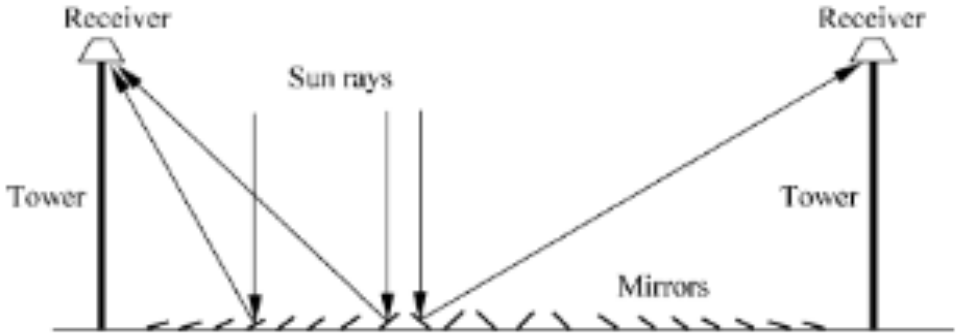


Figure 2-9: Compact Linear Fresnel Reflector

2.4 Applications of Solar Collectors:

Solar collectors are primarily used for heating water for household purposes to reduce the usage and of energy and fossil fuel. Typical application of flat plate solar collector includes the following:

- Water heating for household and residential use like washing clothes, bathing, washing other equipment as well as drinking warm water is done by solar collectors.

- Industrial application of solar water heating includes the use of warm water in leather industry, textile industry, food and beverage industry etc.
- Laundry shops use warm water for washing clothes by using either active or passive collector
- Water of swimming pool is heated using solar collector.
- Solar collectors are used in desalination plants for evaporation of water by heating it to high temperature.
- Solar concentrators are used for solar distillation by heating copper boilers filled with water.
- Solar powered electricity is generated from the radiant energy of the sun using solar collectors.
- Air heater is used for space heating in household and commercial zones.
- Crop drying for agriculture industry is done by forced flow of air using air heater

2.5 Conclusion.

This chapter presents an overview of the existing research on Concentrating and Non concentrating solar collectors providing a fundamental understanding of their operating principles. Flat plate (non-concentrating) and concentrating solar collectors' function by capturing solar radiation and converting it into thermal energy.

Flat plate collectors absorb sunlight directly on a large surface area, transferring heat to a working fluid, typically water or air, for use in residential and industrial heating. In contrast, concentrating solar collectors use optical devices such as parabolic reflectors or Fresnel lenses to focus sunlight onto a smaller absorber area, significantly increasing the operating temperature and efficiency for applications like power generation and industrial heat processes.

Non-concentrating collectors offer simplicity, lower cost, and easy maintenance, making them ideal for widespread domestic and small-scale industrial applications. However, they are limited in terms of temperature range and efficiency. While more efficient at higher temperatures, concentrating collectors require direct normal irradiation, tracking systems and more complex maintenance, making them suitable for regions with high solar insolation and for large-scale thermal energy applications.

In conclusion, the choice between flat plate and concentrating solar collectors depends on factors such as temperature requirements, cost considerations, and available solar resources. Understanding their theoretical performance and efficiency characteristics is essential for optimizing their application in various energy systems. As solar energy continues to be a key solution for sustainable power and heat generation, further advancements in materials, design, and tracking technologies will enhance the efficiency and viability of both collector types.

Chapter 3: Mathematical Model of Solar Parameters.

3.1 Introduction.

The performance analysis of solar collectors relies on accurate mathematical models that describe their thermal and optical behaviour. These models are essential for predicting energy output, optimizing design parameters, and improving efficiency. This chapter presents the mathematical models governing the thermal performance of flat plate solar collectors and concentrating solar collectors.

Many mathematical models have been used to calculate solar radiation, utilizing the available data on meteorological, geographical and climatological parameters. Among these parameters are Sun-Earth angles such as Latitude, Declination, Hour angle, altitude or solar altitude angle, Solar azimuth, Surface azimuth, sunshine hours. These angles define the position of the sun relative to a given location, directly affecting the amount of solar energy received by the collector.

Additionally, sunshine hours play a significant role in determining daily and seasonal global solar irradiation availability in fact, they are the most commonly used parameter.[31] Incorporating meteorological parameters such as air temperature, precipitation, relative humidity, and cloudiness is also crucial for improving the accuracy of solar radiation predictions and collector performance assessment. These parameters influence heat loss, optical efficiency, and thermal storage capabilities in both flat plate solar collectors and concentrating solar collectors.

To make use of these parameters in a practical way, this chapter also introduces an algorithmic approach for solving the mathematical models. These algorithms help simulate and optimize solar collector performance under real-world conditions. By the end of this chapter, the developed models and algorithms will provide a strong foundation for comparing different collector types and selecting the best configuration based on environmental conditions.

3.2 General Information about the Solar Parameters.

Meteorological, geographical and climatological parameters affect the efficiency of solar energy conversion by influencing heat transfer and solar radiation absorption by the solar collectors. Below we shall have a detailed and structured approach to some of the parameters.

3.2.1 Sun -Earth Angles (Geometrical Parameters).

A better understanding of Sun–Earth angles is essential for estimating solar intensity throughout year for any surface at any place with a desired inclination and orientation. These Sun–Earth angles are defined below.

3.2.1.1 Latitude (Φ):

The latitude of an observer (location) on the Earth's surface is the angle made between the radial line joining the observer (location) with the centre of the Earth, and its projection on the equatorial plane as shown in Figure 3-1. For an observer in the northern hemisphere, latitude is positive, whereas for the southern hemisphere it is negative.

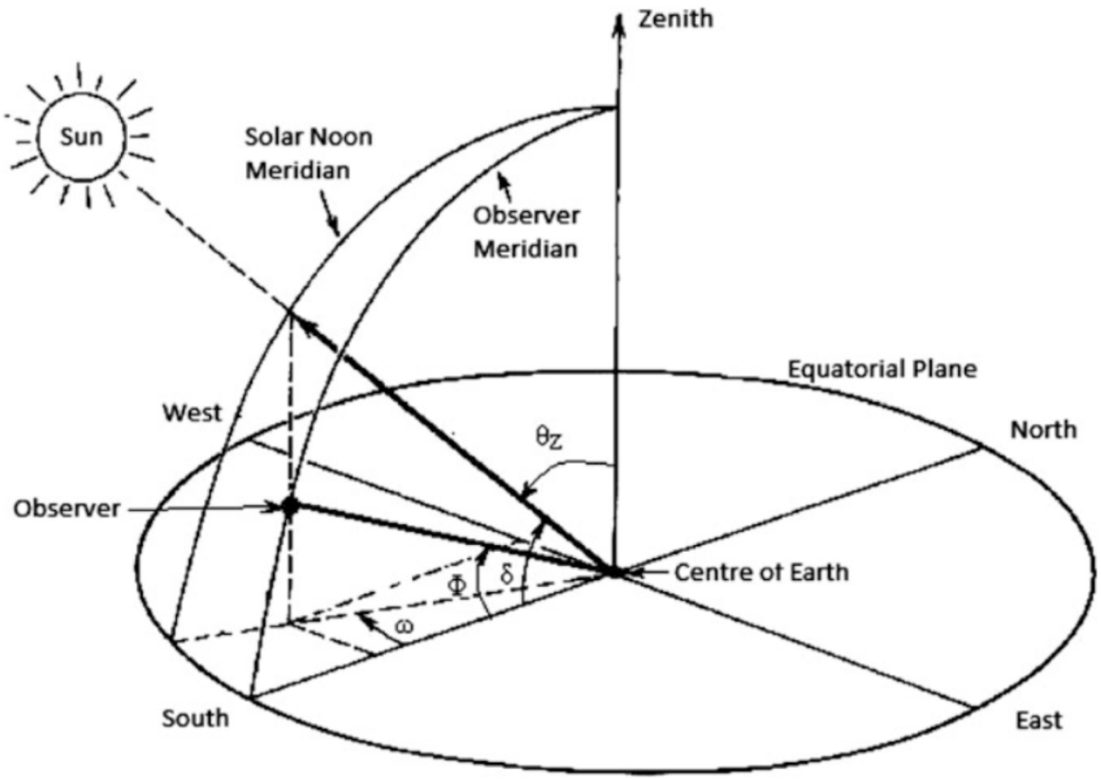


Figure 3-1: View of different sun earth angles

3.2.1.2 Declination (δ):

Declination is defined as the angle between the line joining the centres of the Sun and the Earth, which also determines the direction of the direct rays coming from the Sun and their projection on the equatorial plane as shown in Figure 3-1. Declination is due to the rotation of the Earth around an axis, which makes an angle of either 66.5° with the plane or 23.5° with normal rotation round the Sun as shown in Figure 3-1.

The declination is calculated by the following relation

$$\delta = 23.45° \, sin\left(\frac{360}{365}(284 + n)\right) \qquad (3\text{-}1)$$

n ; day of the year starting from 1st January

We note that;

$\delta > 0$ for the summer and spring.s

$\delta < 0$ for the Autumn and Winter.

Always: $-23°.45 \leq \delta \leq 23°.45$

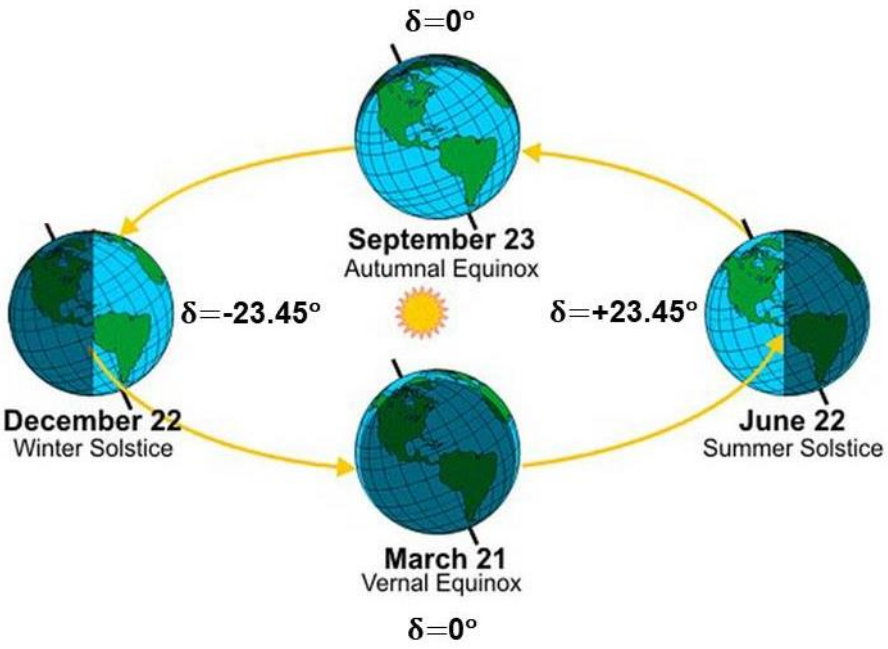


Figure 3-2: minimum and maximum values of declination

3.2.1.3 Hour Angle (ω):

This is the angle between projections of the Sun's rays (solar meridian) and the line running south–north through centre. The south–north line is also referred to as the "line due south."

In other words, the hour angle is defined as the angular displacement of the Sun from the local meridian because of the Earth's rotation around its own axis. The hour angle corresponding to 1 h is 15°.

$$\omega = (ST - 12) \times 15° \qquad (3\text{-}2)$$

where ST is the local solar time.

The total hour angle from sunrise to sunset is (2ω)

The sign $\pm\boldsymbol{\omega}_s$ for the hour angle is taken as a negative for morning and positive at afternoon.

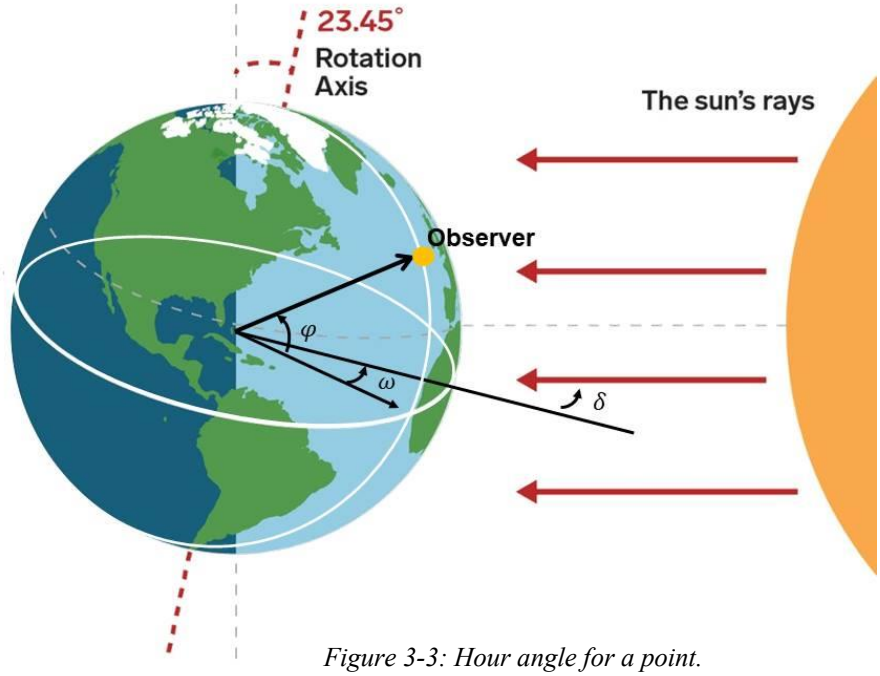


Figure 3-3: Hour angle for a point.

3.2.1.4 The Height of The Sun (h):

It is the angle that the direction of the sun makes with the horizontal plane. It is calculated by the following relation

$$sin(h) = (sin(L) \times sin(\delta)) + (cos(L) \times cos(\delta) \times cos(\omega)) \qquad (3\text{-}3)$$

ω: Hour angle

δ: Declination

L: Latitude

3.2.1.5 Zenith Angle (θ_Z):

The angle between Sun's rays and the line perpendicular to a horizontal plane is known as the "zenith angle" θ_Z (Figure 3-1).

$$\Theta_Z = 90° - h \qquad (3\text{-}4)$$

Where h is the height of the sun.

3.2.1.6 Altitude Or Solar Altitude Angle (αs):

The angle made between a horizontal plane and the Sun's rays is known as the "altitude angle." Referring to Figure 3-4.

3.2.1.7 Slope (β):

This is the angle between the plane surface under consideration (of the solar collector) and the horizontal surface (tangential plane at observer), Figure 3-4. Its numerical value is considered positive for slope toward the south and negative for slope toward the north.

3.2.1.8 Surface Azimuth Angle (γ):

The angle made between the line due south and the projection of normal to the inclined surface on the horizontal plane (tangential plane at observer on the surface of the Earth, Figure 3-4 is termed the "surface azimuth angle." In the northern hemisphere, conventionally γ is negative (positive for the southern hemisphere) for projections in east of south and positive (negative for southern hemisphere) for projections falling west of south.

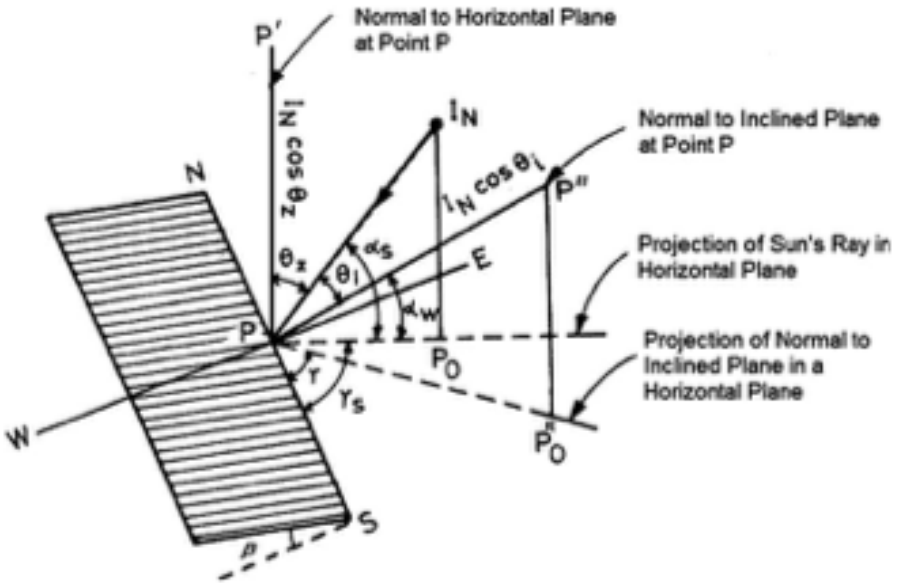


Figure 3-4: View of various sun earth angles on an inclined surface

3.2.1.9 Solar Azimuth Angle (γ_S):

The angle made between the projection of beam radiation on the horizontal plane and the line due south is known as the "solar azimuth angle" (Figure 3-4). The sign convention of the solar azimuth angle is the same as the sign convention of the surface azimuth angle.

It is given by the following relation:

$$sin(\gamma s) = \frac{cos(\delta) \times sin(\omega)}{cos(h)} \quad (3\text{-}5)$$

γs: Solar azimuth angle

ω : Hour angle

δ : Angle of declination

Note:

$\gamma s > 0$: when the sun is located on the west

$\gamma s < 0$: when the sun is located on the east

$\gamma s = 0$: when the sun is located on the south plane

3.2.1.10 Angle of Incidence (θ_i):

The angle made between normal to the inclined surface and the solar beam radiation falling on the inclined surface is known as the "angle of incidence" (Figure 3-4). In general, the angle of incidence θ_i can be expressed as,

$$\begin{aligned} cos\,\theta_i = {} & \sin\delta \sin\varphi \cos\beta \\ & - \sin\delta \cos\varphi \sin\beta \cos\gamma \\ & + \cos\delta \cos\varphi \cos\beta \cos\omega \\ & + \cos\delta \sin\varphi \sin\beta \cos\gamma \cos\omega + \cos\delta \sin\beta \sin\gamma \sin\omega \end{aligned} \quad (3\text{-}6)$$

For a horizontal plane facing due south, $\gamma = 0, \beta = 0,\ \theta_i = \theta_z(Zenith\ angle)$

$$cos\,\theta_z = cos\,\varphi\, cos\,\delta\, cos\,\omega + sin\,\delta\, sin\,\varphi \quad (3\text{-}7)$$

Referring to Figure 3-1, the zenith angle (θ_z) will be 90° in the morning as well as in the evening before sunrise and after sunset and $\omega = \omega s$ thus the equation can be written as follows

$$0 = cos\,\varphi\, cos\,\delta\, cos\,\omega s + sin\,\varphi\, sin\,\delta \quad (3\text{-}9)$$

$$\omega s = cos^{-1}(-tan\,\varphi\, tan\,\delta) \quad (3\text{-}8)$$

As mentioned previously, 1h =15°; hence, the number of daylight (sunshine) hours (N) is given by

$$N = \frac{2}{15} cos^{-1}(tan\,\varphi\, tan\,\delta) \qquad (3\text{-}10)$$

The variation of N with the nth day of the year for different latitudes in the Northern hemisphere is shown in Figure 3-2.

3.2.1.11 Sunshine Hour (N):

The total duration in hours of the Sun's movement from sunrise to sunset. It is defined in terms of the hour angle as

$$\boldsymbol{N} = \frac{2\omega s}{15} \qquad (3\text{-}11)$$

Here 1h = 15°

3.3 Solar Time and Duration of the Day.

3.3.1 Duration of the Day.

To get the length of the day we calculate the hour angle at sunset knowing that the sunset and sunrise corresponds to a height of the sun (h) zero.

Suppose h = 0 therefore one finds the sunset hour angle with the following relation:

$$\omega s = arc\cos[-tg(\varphi) \times tg(\delta)] \qquad (3\text{-}12)$$

ωs: Hour angle at sunset

δ : angle of Declination

φ: Latitude of the earth

Therefore:

The sunshine hour for sunrise is given by the equation:

$$(ST)_{sunrise} = 12 - \frac{\omega s}{15} \qquad (3\text{-}13)$$

The sunshine hour for sunset is also given by the equation:

$$(ST)_{sunset} = 12 + \frac{\omega s}{15} \qquad (3\text{-}14)$$

3.3.2 Solar Time.

The is the time according to the apparent movement of the sun in the sky considering the hour at which the sun crosses the local meridian solar noon. Solar time does not consider local clock time.

The equation which relates Solar time with the legal time is

$$ST = LT + ET + 4(L_{ST} - L_{Loc}) \quad (3\text{-}15)$$

Where:

ST: Solar Time

LT: Local standard Time

L_{Loc}*: Longitude of the location*

L_{ST}*: is the standard meridian for a local zone (*$L_{ST} = 15° \times \Delta\ Greenwich\ MT(Time)$)

This value is negative for places west of the Greenwich meridian and positive for places east of the Greenwich meridian.

ET: is the equation of time given by:

$$ET = 229.2(0.000075 + O.OO1868\cos B - 0.032077\sin B - 0.014615\cos 2B - 0.04089\sin 2B) \quad (3\text{-}16)$$

Where:

$$B = \frac{360(n-1)}{365} \quad (3\text{-}17)$$

Where n is between $1 \leq n \leq 365$ *the number of days in a year sometimes called Julian day n can be easily calculated from Table 1.1.*

One should note that ET (Equation of Time) is a measure of the slight variation in the length of each day depending on the time of the year Over the year, solar time can deviate from the time shown by clocks by more than 15 minutes. Estimation of solar time is tightly connected to solar irradiance evaluation. It's used in all of the sun-angle relationships. Whereas, the meantime is never used in these calculations.

Table 3-1 Values Julian's day by month.

Month	*n* for *i*th Day of Month
January	i
February	$31 + i$
March	$59 + i$
April	$90 + i$
May	$120 + i$
June	$151 + i$
July	$181 + i$
August	$212 + i$
September	$243 + i$
October	$273 + i$
November	$304 + i$
December	$334 + i$

Table 3-2 Latitude, longitude, and elevation for different places in the world.

Place	Latitude (φ)	Longitude (l_{loc})	Elevation (E_o) (mean sea level)
New Delhi	28° 35'N	77° 12'E	216 m above msl
Mumbai	18° 54'N	72° 49' E	11 m above msl
Chennai	13° 00' N	80° 11' E	16 m above msl
Kolkata	22° 32' N	88° 20' E	6 m above msl
London	51° 30' N	00° 07' W	35 m above msl
New York	40° 42' N	74° 00' W	10 m above msl
Paris	48° 51' N	02° 21'E	35 m above msl
Moscow	55° 45' N	37° 37'E	156 m above msl
Singapore	01° 17' N	103°50' E	6 m above msl
Beijing	39°54' N	116° 23'E	50 m above msl
Berlin	52° 31' N	13°23'E	34m above msl

3.4 Solar Radiation.

Solar radiation, while passing from the extraterrestrial region to the terrestrial region through the Earth's atmosphere, suffers scattering losses and atmospheric absorption. After absorption by the atmosphere, the rate of normal solar flux (normal solar radiation/irradiance) reaching the Earth's surface is determined by

$$I_N = I_{on} \times exp[-(m.\varepsilon.T_R + \alpha)] \quad (3\text{-}18)$$

I_N ; is the normal solar radiation

I_{on} ; is the extraterrestrial radiation on the earth's surface

m; is the air mass given by the equation;

$$m = [\cos\theta_z + 0.15 \times (93.885 - \theta_z)^{-1.253}]^{-1} \quad (3\text{-}19)$$

T_R ; Is the turbidity factor also defined as the cloudiness factor for the lumped atmosphere.

α ; is known as lumped atmospheric parameter which accommodates further attenuation of direct normal irradiance in the terrestrial zone.

ε ; is the expression known as the integrated optical thickness of the terrestrial clear and dry atmosphere/ Rayleigh atmosphere.

3.4.1 Beam Radiation (I_b):

This is a normal component of solar radiation (normal irradiance) in W/m^2 propagating along the line joining the receiving surface and the Sun on a horizontal/inclined surface. It has a direction and also termed "direct radiation."

3.4.2 Diffuse Radiation (I_d):

This is the solar radiation (in W/m^2) scattered by aerosols and other particulates; diffuse radiation does not have any definite direction.

3.4.3 The Total Radiation (I):

This is the sum of the beam (direct) and diffuse radiation in W/m^2. It is also known as "global radiation."

$$I = I_b + I_d \qquad (3\text{-}20)$$

3.5 Irradiation (Radiant Exposure):

The incident solar radiation/irradiance on a surface in J/m^2 per hour or per day is known as "irradiation." It is obtained by integrating beam/diffuse/total radiation over 1 h or day.

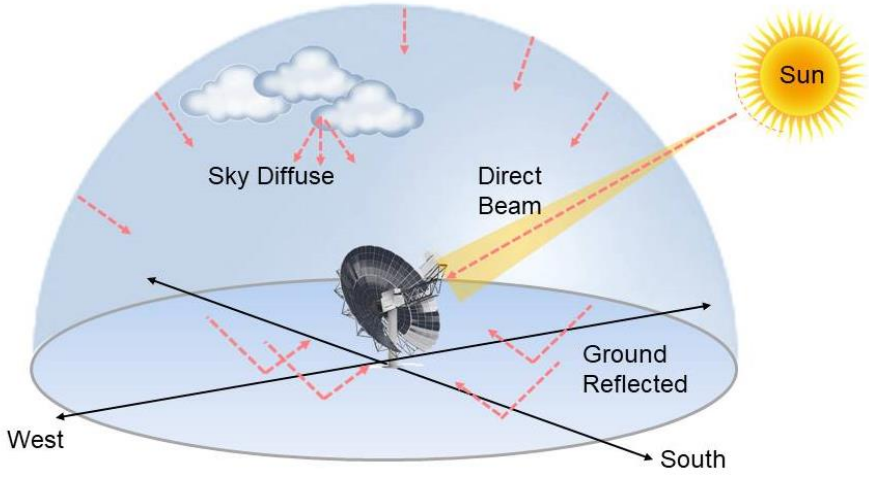


Figure 3-5: Direct, Reflected and Beam radiations

Due to elliptical orbit of the Earth's motion around the Sun, the Sun–Earth distance is not fixed but rather varies around the year, and the maximum variation is up to 1.7 %. The solar intensity (solar radiation/solar irradiance) in the extraterrestrial region has been measured (by NASA through satellite). For the nth day of the year, the solar intensity on a plane perpendicular to the direction of solar radiation is given by;

$$I_{on} = I_{sc}\left[1 + 0.033cos\left(\frac{360n}{365}\right)\right] \quad (3\text{-}21)$$

I_{on} *: is the extraterrestrial radiation on the earth's surface*

n: n^{th} day of the year starting from 1st January

I_{SC}*: is the solar constant defined as the radiant solar (energy) flux received in the extraterrestrial region on a plane of unit area kept perpendicular to the solar radiation at the mean Sun–Earth distance. The value of solar constant is 1367 W/m^2.*

The radiation emitted by the sun varies slightly over defined periods; for our part, we assume the radiation emitted by the sun to be constant and we are only interested in the influence of the distance on the energy received by the earth.

3.6 Solar Radiation Incident on a Horizontal Surface.

3.6.1 Extraterrestrial Region.

3.6.1.1 Instantaneous Radiation (I_{oh}):

Here, the solar radiation (I_{oh}) incident on a horizontal plane in the extraterrestrial region/outside the atmosphere in W/m^2, which is equivalent to being in the absence of atmosphere, is a component of (I_{on}) along the normal to horizontal surface and can be obtained from equations (3-21) and as follows:

$$I_{oh} = I_{on}\cos(\theta_z) = I_{on}\sin(h) \quad (3\text{-}22)$$

Where:

h: Height of the sun.

θ_z*: Zenith angle.*

I_{on} *; is the extraterrestrial radiation on the earth's surface*

3.6.2 Hourly Irradiation (Radiation Received in Hourly Time Intervals).

The extraterrestrial radiation on a horizontal surface for a given period from hour angles ω_1 to ω_2 (where ω_2 is larger) can be calculated for a period, and it is given by

$$I'_{oh} = \frac{12 \times 3600}{\pi} I_{on}[\cos\varphi\cos\delta\,(\sin\omega_2 - \sin\omega_1) + \frac{\pi(\omega_2 - \omega_1)}{180}\sin\varphi\sin\delta] \quad (3\text{-}23)$$

With:

I'_{oh}*: Hourly irradiation*

δ*: Angle of declination of the sun*

φ*: Latitude of the place*

ω_1, ω_2*: Hourly angles corresponding to the two solar times*

3.6.3 Daily Extraterrestrial Irradiation (H_o):

For calculations of daily solar radiation on a horizontal surface in the extraterrestrial region H_o in J/m^2, can be obtained from the equation.

$$H_o = \frac{24 \times 3600}{\pi} I_{on}\left(\cos\varphi\cos\delta\sin\omega_s + \frac{2\pi\omega_s}{360}\sin\delta\sin\varphi\right) \quad (3\text{-}24)$$

With:

H_o*: Daily irradiation [J/m²]*

φ*: Latitude of the place*

δ*: Declination angle of the sun.*

ω_s*: Hourly angle at sunset*

3.6.4 The Monthly Average Daily Extraterrestrial Radiation ($\bar{H}_o$):

This represents the average daily radiation for each month in a year, in order to avoid calculating daily radiation of each day we calculate using day types for each month.

Table 3-3 The day types of each month

Month	01	02	03	04	05	06	07	08	09	10	11	12
Day Type	17	16	16	15	15	11	17	16	15	15	14	10

3.6.5 Terrestrial Region.

The hourly total solar radiation $\boldsymbol{I_h}$ is the sum of beam/direct and diffuse radiation on a horizontal surface in the terrestrial region and is written as

$$\boldsymbol{I_h} = I_b + I_d \qquad (3\text{-}25)$$

In addition, the hourly total solar radiation in W/m^2 can be calculated from known daily solar radiation data in J/m^2.

Collares Pereira and Rabl [32] proposed the following model to determine the hourly total global solar radiation from known daily solar radiation data in J/m^2:

$$\boldsymbol{I_h} = R_t H_o \text{ (J /m}^2 \text{ h)} \qquad (3\text{-}26)$$

$$R_t = \frac{\pi}{24}(a + b \times \cos\omega)\frac{\cos\omega - \cos\omega_s}{\sin\omega_s - \frac{\pi\omega}{180}\cos\omega_s} \qquad 3\text{-}27)$$

The coefficients a and b are given by

$$a = 0.409 + 0.5016\sin(\omega_s - 60) \qquad (3\text{-}28)$$

$$b = 0.6609 - 0.4767\sin(\omega_s - 60) \qquad (3\text{-}29)$$

Where ω is the hour angle in degrees for the time in question, and ω_S is the sunset-hour angle.

The daily total solar radiation (H) in J/m^2 on a horizontal surface in the terrestrial region can be written as

$$H = \sum_{t=1}^{t=N} \boldsymbol{I_h} \times 3600 \qquad (3\text{-}30)$$

The average monthly total solar radiation ($\overline{H}$) in J/m^2 on a horizontal surface in the terrestrial region can be written as

$$\overline{H} = \frac{\sum_i^{n_o} H_i}{n_o} \qquad (3\text{-}31)$$

3.7 Evaluation Of the Parameters Used for Solar Radiation.

3.7.1 The Monthly Average of Daily Total Radiation ($\overline{H}$) In J/m^2 on a Horizontal Surface.

The monthly average of daily solar radiation ($\overline{H}$)in J/m^2 available on a horizontal surface can be calculated using following **Prescott Angstrom empirical model**: [33]

$$\frac{\overline{H}}{\overline{H_o}} = a + b\left(\frac{\overline{n}}{\overline{N}}\right) = a + b\bar{\sigma} = \overline{K_t} \qquad (3\text{-}32)$$

where $\overline{n}$ and $\overline{N}$ are the observed monthly average of daily bright sunshine hours and the total length of average days of month. $\overline{H}$ and $\overline{H_o}$ are the monthly average of daily total solar radiation on a horizontal surface in the terrestrial and extraterrestrial region, respectively.

The regression coefficients a and b are given by

$$a = -0.309 + 0.539\cos\varphi - 0.0693E_o + 0.290\left(\frac{\overline{n}}{\overline{N}}\right) \qquad (3\text{-}33)$$

and

$$b = 1.527 - 1.027cos\varphi + 0.0926E_o - 0.359\left(\frac{\overline{n}}{\overline{N}}\right) \qquad (3\text{-}34)$$

where φ *is latitude of the place, and* E_O *is the height of the place (in kilometres) above sea level (Table 3-2 The elevation of the location above sea level is in kilometres.)*

$\bar{\sigma}$ *: is the monthly fraction of sunshine*

3.7.1.1 The Daily clearness index K_T

A daily clearness index K_T is the ratio of daily solar radiation (Equation 3-30) on a horizontal surface in the terrestrial region to daily solar radiation on a horizontal surface (Equation 3-24) in the extraterrestrial radiation for that day.

$$K_T = \frac{H}{H_o} \qquad (3\text{-}35)$$

where H is measured daily total solar radiation, and H_O *is obtained from (Equation 3-24).*

3.7.2 Estimation of Beam and Diffuse Components of Daily Solar Radiation.

If we know K_T, the daily solar radiation in J/m^2 on a horizontal surface can be obtained from Equation (3-35). The separation of daily solar radiation, H, on a horizontal surface into its beam and diffuse components is important to classify weather conditions.

If $\frac{H_d}{H}$ is the ratio of daily diffuse radiation to daily total solar radiation, a correlation was proposed in terms of K_T by **Collares -Pereira and Rabl [32]** as follows

$$\frac{H_d}{H} = 0.99 \qquad \text{for } K_T \leq 0.17$$

$$\frac{H_d}{H} = 1.188 - 2.72K_T + 9.473K_T^2 - 21.865K_T^3 + 14648K_T^4 \qquad \text{for } 0.17 < K_T < 0.75$$

$$\frac{H_d}{H} = -0.5K_T + 0.632 \qquad \text{for } 0.75 < K_T < 0.80$$

$$\frac{H_d}{H} = 0.2 \qquad \text{for } K_T \geq 0.8 \qquad \textit{(3-36)}$$

Reindl et al. also developed a correlation to predict the daily diffuse radiation fraction $\frac{H_d}{H}$ based on the clearness index (K_T). The model accounts for non linear behavior of solar radiation under various atmospheric conditions, offering better accuracy compared to the **Collares - Pereira** and **Rable model**.

$$\begin{cases} \frac{H_d}{H} = 1.0 & \text{for } K_T \leq 0.3 \\ \frac{H_d}{H} = 1.390 - 4.027K_T + 5.531K_T^2 - 3.108K_T^3 & \text{for } 0.3 < K_T < 0.78 \\ \frac{H_d}{H} = 0.15 & \text{for } K_T > 7.8 \end{cases} \qquad \textit{(3-37)}$$

3.7.3 Monthly average clearness index $\overline{K}_T$

The monthly average clearness index, $\overline{K}_T$, is the ratio of monthly average solar radiation on a horizontal surface *Equation 3-31*, in the terrestrial region to the monthly average extraterrestrial solar radiation.

$$\overline{K}_T = \frac{\overline{H}}{\overline{H}_o} \qquad \textit{(3-38)}$$

Where $\overline{H}$ is the measured monthly solar radiation and $\overline{H}_o$ is given by Equation 3-24 for n given in Table 3-1.

3.7.4 Estimation of the monthly average of daily diffuse solar radiation on a horizontal surface.

For a known $\overline{K}_T$, and sunset hour angle ω_s, the monthly average daily diffuse solar radiation on a horizontal surface can be estimated as proposed by the **Collares -Pereira and Rable** [32] correlation model.

$$\frac{\overline{H}_d}{\overline{H}} = 0.775 + 0.00653(\omega_s - 90) - [0.505 + 0.00455(\omega_s - 90)]\cos[115\overline{K}_T - 103] \quad (3\text{-}39)$$

Another correlation to predict the monthly average of daily diffuse solar radiation on a horizontal surface is as follows;

$$\frac{\overline{H}_d}{\overline{H}} = 1.39 - 4.027\overline{K}_T + 5.531\overline{K}_T^2 - 3.108\overline{K}_T^3 \quad (3\text{-}40)$$

3.7.5 Estimation of the monthly average hourly direct solar radiation.

This can be estimated from the following relation;

$$\overline{H}_b = \overline{H} - \overline{H}_d \quad (3\text{-}41)$$

Where; $\overline{H}$ is the of monthly average solar radiation on a horizontal surface in the terrestrial region.

$\overline{H}_d$ is the monthly average diffuse solar radiation on a horizontal surface.

3.7.6 Diffuse hourly solar radiation in monthly average.

$$\bar{I}_d = \overline{H}_d \times R_d \quad (3\text{-}42)$$

$$R_d = \frac{\pi}{24}\left[\frac{\cos\omega - \sin\omega_s}{\sin\omega_s - \frac{\pi\omega_s}{180}\cos\omega_s}\right] \quad (3\text{-}43)$$

Where R_d is the conversion factor for diffuse radiation in monthly averages.

$\overline{H}_d$ is the monthly average diffuse solar radiation on a horizontal surface.

3.7.7 Direct hourly solar radiation in monthly average.

$$\bar{I}_b = \bar{I}_h - \bar{I}_d \quad (3\text{-}44)$$

3.8 Estimation of Solar Radiation on an Inclined/Tilted Surface.

3.8.1 Conversion Factors.

There are three types of solar radiation for any inclined surface namely, beam, diffuse and reflected solar radiation from a horizontal surface and the surfaces surrounding it.

Therefore, there are three conversion factors, namely, for beam (R_b), for diffuse (R_d), and for reflected (R_r) solar radiations.

These conversion factors convert the beam and diffuse solar radiations of a horizontal surface to those of an inclined surface. These conversion factors are as follows:

3.8.2 Conversion factor for beam solar radiation.

The conversion factor for beam radiation (R_b) is defined as the ratio of beam radiation incident on an inclined surface I_{bT} in W/m^2 to that incident on a horizontal surfaceI_b in W/m^2,

$$R_b = \frac{I_{bT}}{I_b} = \frac{\cos\theta_i}{\cos\theta_Z} \quad (3\text{-}45)$$

$$R_b = \frac{\cos\theta_i}{\cos\theta_z}\left(1 - \frac{R_d}{R_t}.\frac{H_d}{H}\right) + \frac{1}{2}(1+\cos\beta)\frac{R_d}{R_t}.\frac{H_d}{H} + \frac{1}{2}\rho(1-\cos\beta) \quad (3\text{-}46)$$

where;

θ_Z and θ_i are the angles of incidence on the horizontal and inclined, surfaces respectively

Depending on the orientation of inclined surface, the expression for cos θ_i and cos θ_Z can be obtained from equations (3-6) and (3-7*)*, respectively;

β: is the angle of inclination

ρ: is the reflection coefficient (albedo), 0.2 for ordinary ground and 0.6 for snow covered ground.

R_t : is the conversion factor for the hourly monthly average global radiation on a horizontal surface.

R_d : is the conversion factor for diffuse radiation

$\frac{H_d}{H}$ is the ratio of daily diffuse radiation to daily total solar radiation

3.8.3 Conversion factor for Diffuse solar radiation.

The conversion factor for diffuse radiation (R_d) is defined as the ratio of diffuse radiation incident on an inclined surface in W/m^2 to that on a horizontal surface in W/m^2

Diffuse radiation can be estimated by considering the sky as the isotropic source of diffuse radiation. For a tilted surface at an angle β from the horizontal surface, the conversion factor for diffuse radiation is given as follows:

$$R_d = \frac{1+\cos\beta}{2} \quad 3\text{-}47)$$

3.8.4 Conversion factor for Reflected solar radiation.

Reflected solar radiations are the radiations reflected from the ground and other objects near the surface. If one assumes that reflected radiations are diffuse and isotropic, the conversion factor for reflected solar radiation (R_r) is given by;

$$R_r = \frac{1-\cos\beta}{2} \quad (3\text{-}48)$$

3.8.5 Conversion factor of hourly total solar radiation on an Inclined/Tilted surface.

This is the ratio of hourly total solar radiation incident on an inclined/tilted (I_T) surface to that on a horizontal surface, $(\boldsymbol{I_h})$. It is calculated as follows:

$$R = \frac{I_T}{I_h} \tag{3-49}$$

3.8.5.1 For the conversion factor of monthly average hourly total solar radiation on an inclined surface the equation becomes.

$$\bar{R} = \frac{\bar{I}_T}{\bar{I}_h} = \frac{\cos\bar{\theta}_i}{\cos\bar{\theta}_z}\left(1 - \frac{R_d}{R_t}.\frac{\bar{H}_d}{\bar{H}}\right) + \frac{1}{2}(1+\cos\beta)\frac{R_d}{R_t} + \frac{1}{2}\rho(1-\cos\beta) \tag{3-50}$$

3.8.6 Conversion factor for daily total solar radiation on an inclined surface.

$$R' = \frac{H_T}{H} = \left(1 - \frac{H_d}{H}\right)R'_b + \frac{1}{2}\frac{H_d}{H}(1+\cos\beta) + \frac{1}{2}\rho(1-\cos\beta) \tag{3-51}$$

3.8.7 Conversion factor for monthly average daily total solar radiation on an inclined surface.

$$\bar{R}' = \frac{\bar{H}_T}{\bar{H}} = \left(1 - \frac{\bar{H}_d}{\bar{H}}\right)\bar{R}'_b + \frac{1}{2}\frac{\bar{H}_d}{\bar{H}}(1+\cos\beta) + \frac{1}{2}\rho(1-\cos\beta) \tag{3-52}$$

$\bar{H}_T$: is the monthly average daily total solar radiation on an inclined surface.

$$\bar{R}'_b = \frac{[\cos(L-\beta)\cos(\delta)\sin(\omega'_s)] + \left[\frac{\pi}{180}\omega'_s\sin(L-\beta)\sin(\delta)\right]}{[\cos(\delta)\cos(L)\sin(\omega'_s)] + \left[\frac{\pi}{180}\omega'_s\sin(\delta)\sin(L)\right]} \tag{3-53}$$

With

$$\omega'_s = min[\cos^{-1}(\tan(L)\times\tan(\delta))\,;\cos^{-1}(-\tan(L-1)\times\tan(\delta))] \tag{3-54}$$

3.9 Total solar radiation on an Inclined/Tilted surface.

For any inclined surface, Liu and Jordan [34] estimated total solar radiation using the following relation;

$$I_T = I_b R_b + I_d R_d + \rho R_r (I_b + I_d) \tag{3-55}$$

Substituting for R_d and R_r from equations (3-47) and (3-48) respectively the equation becomes;

$$I_T = I_b R_b + I_d \left(\frac{1+\cos\beta}{2}\right) + (I_b + I_d)\rho \left(\frac{1-\cos\beta}{2}\right) \quad (3\text{-}56)$$

Where;

β: is the angle of inclination

ρ: is the reflection coefficient (albédo), 0.2 for ordinary ground and 0.6 for snow covered ground.

I_b: is the hourly direct (beam) solar radiation on a horizontal surface.

I_d: is the hourly diffuse solar radiation on a horizontal surface.

3.9.1 Monthly Average Daily Solar Radiation $\bar{H}_T$ on Inclined Surface.

$$\bar{H}_T = (\bar{H} - \bar{H}_d)\bar{R}_b + \bar{H}_d \left(\frac{1+\cos\beta}{2}\right) + \rho\bar{H} \left(\frac{1-\cos\beta}{2}\right) \quad (3\text{-}57)$$

Where;

$\bar{R}_b$: is the conversion factor for average daily beam radiation

Chapter 4: Algorithm and Computational Program using Matlab.

Matlab is a numerical computational software package marketed by MathWorks. It was originally developed in the late 1970s by Cleve Moler, a professor of mathematics at the University of New Mexico.

The Matlab programming language, derived from Fortran, has evolved to include many powerful and practical graphical and analytical tools. It has become an important platform for engineering and science education, as well as for research.

Matlab is a valuable first programming language, and for many it will be the most preferred language.

Matlab offers many advantages over conventional computer languages (e.g., C, Fortran, Pascal…) for solving technical problems.

Matlab is an interactive system whose basic data element is an array that does not require dimensioning.

Once you enter Matlab, the main tools within or accessible from the desktop are:

- The Command Window.
- Command History.
- The Workspace.
- The Current Directory.
- The Help Browser.
- The Start button.

Not all commands executed in the Command Window can be saved and re-executed multiple times. Therefore, another method for repetitive operation with Matlab is:

a) Create a file with a list of commands.

b) Save the file, and

c) Run the file.

If necessary, corrections or modifications can be made to the commands in the file. The files used for this purpose are called script files.

In our work, we use Matlab as a support tool to execute the program which calculates hourly global solar irradiance across various geographical regions, the different geographical locations considered include;

- Stockholm, Sweden-High Latitude region
- Entebbe Uganda -Equatorial Region
- Bloemfontein, South Africa -Subtropical
- Ghardaïa, Algeria- Semi Arid Région

Below are the steps to execute the Matlab program.

1. Input parameters;
    - Location name
    - Latitude
    - Longitude
    - Time Zone
    - Solar constant: 1367W/m^2
    - Angström coefficients (region specific a, b)

2. Sunshine Duration Estimation.
   To estimate sunshine hours(N), the algorithm first calculates the solar declination (δ) Equation (3-1) and sunset hour angle ω_s Equation (3-9) for the day June 15th which is n =166
   The maximum possible sunshine duration is then computed using Equation (3-11)

The day is divided into 30-minute intervals and a binary indicator is used to approximate sunshine presence based on sunrise and sunset times. Summing these intervals provides the daily sunshine duration N.

3. Daily Extraterrestrial Radiation Estimation
   Using the Angström- Prescott model, global daily radiation (H) is estimated using from sunshine duration and extraterrestrial radiation (H_o)
    - Calculate inverse relative earth-sun distance Equation (3-21)
    - Calculate daily extraterrestrial radiation Equation (3-24)

4. Estimate Terrestrial Global Radiation (H).

    - Use Angstrom Prescott model and the different values of Angstrom coefficients a, b for the various geographical locations Equation (3-32)

Both H and H_O are converted from MJ/m^2 to W/m^2 by dividing by the number of seconds in a day (86400s).

5. Estimate Hourly Solar Radiation using Collares Pereira and Rabl Model for the different geographical regions
    - Solar time correction: The difference between solar time and local standard time is calculated using the Equation of time and the longitude correction Equation (3-15), Equation (3-16)

    - Hourly angles: The hour angle is computed for each hourly midpoint Equation (3-2), Equation (3-9)

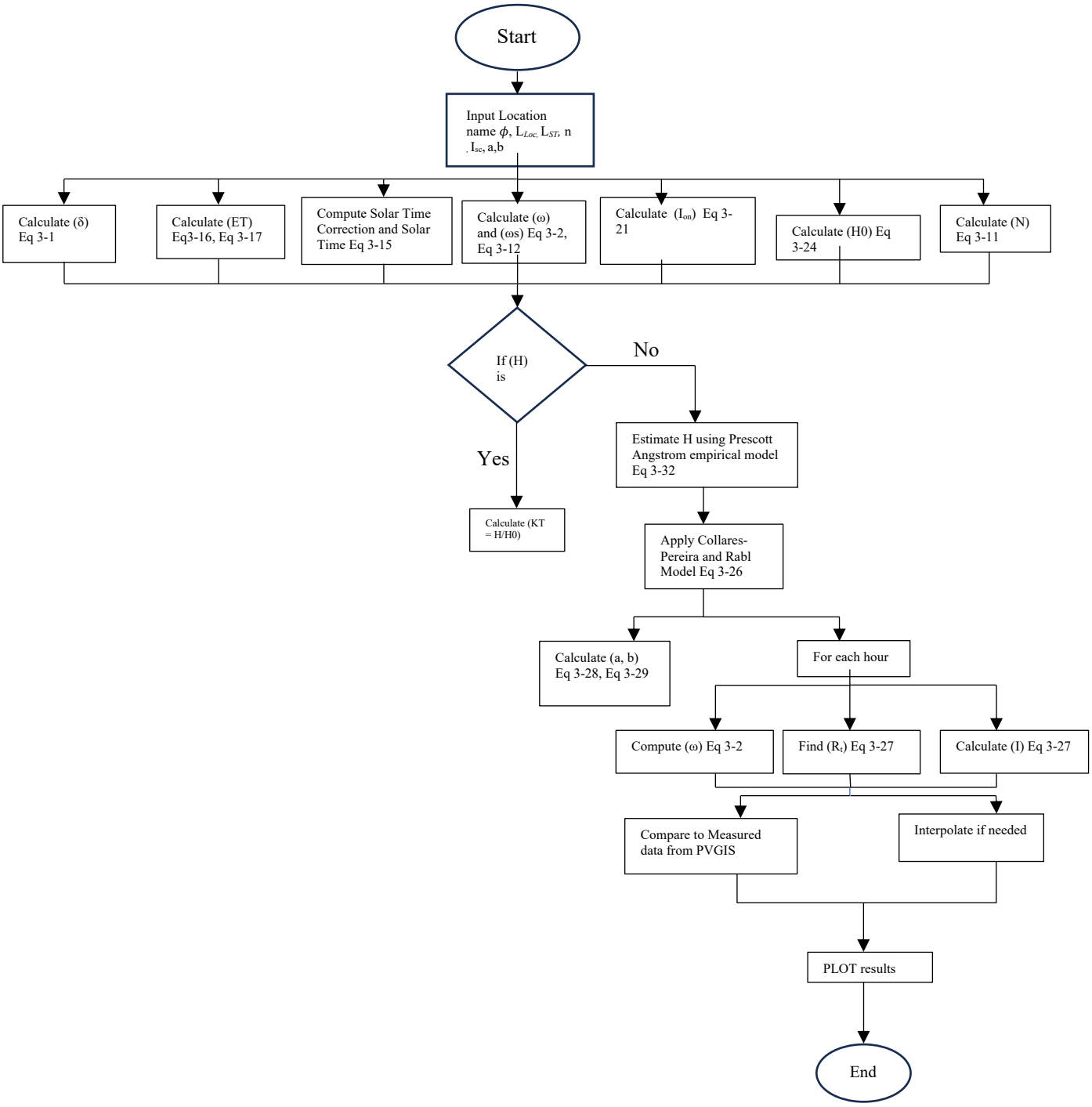
    - Hourly Radiation fraction is calculated from the following equations Equation (3-26), Equation (3-27), Equation (3-28), Equation (3-29)

- This yields the hourly global radiation in W/m^2 by converting from $MJ/m^2/h$ and stored for visualization.

6. PVGIS Data Synchronization.

   To compare the modeled radiation with real measurements, hourly global radiation data from PVGIS was obtained in Coordinated Universal Time, this data is shifted to local solar time.
   The resulting time aligned PVGIS data enables a direct comparison with the modeled values
7. Validation and Plotting.
   A representative day (June 15) was selected to compare modeled radiation against PVGIS data.
   The plots of hourly global radiation showed agreement between the two datasets.

4.1 The flowchart of the calculation program.



4.2 Conclusion.

The chapter explained how the Matlab algorithm was developed to calculate hourly solar irradiance, starting from the basic formulas all the way to the final model results.

It also presented a flowchart to visualize the step-by-step process of the Matlab Calculation from collecting input data, running the necessary calculations and then producing useful outputs.

In addition, the main procedures of the algorithm and the key formulas used to estimate different components of solar irradiance such as beam, diffuse and global radiation were discussed. These calculations are essential for understanding how much solar energy is available at a given location and time.

Chapter 5: Results and Discussions.

5.1 Validation of the model.

In this study, the solar irradiation of the implemented model is validated using data from Photovoltaic Geographical Information System (PVGIS) database[35] of three geographically and climatically distinct cities: Entebbe (Uganda), Stockholm (Sweden) and Bloemfontein (South Africa).

These locations are deliberately chosen to represent equatorial high-latitude northern and mid-latitude southern climates. This diverse selection ensures that the model is tested across a wide range of solar radiation profiles, ambient temperatures and seasonal variability which are essential factors influencing collector performance.

The comparison is performed on an hourly basis across representative day for the month May 20th for the three cities by checking how well the model matches the experimental data in each location.

5.1.1 Entebbe, Uganda (0.06°N, 32.44°E).

Entebbe is located near the equator and experiences relatively uniform solar radiation and daylight hours throughout the year. Seasonal variation is minimal with cloud cover during the wet seasons being the primary factor influencing radiation levels. The validation in Entebbe helps assess the model's performance under consistent solar exposure.

The model is evaluated for Entebbe Uganda on May 20th using a tilt angle of 0° and an azimuth of 180°. The model's calculated global irradiance (W/m²) is compared against PVGIS reference data across a 24-hour solar time period.

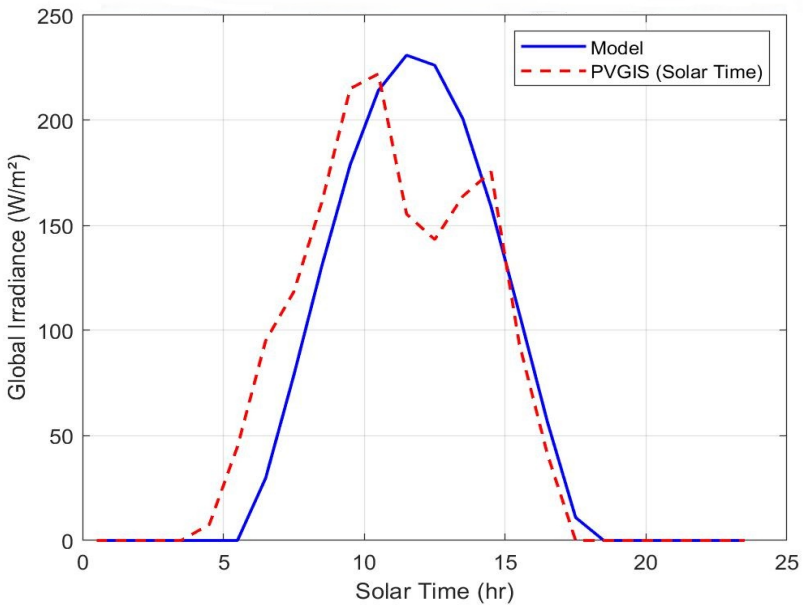


Figure 5-1 Comparison between analytical Model and calculated data (PVGIS) for Entebbe on 20th May

Both the model (solid blue line) and PVGIS data (dashed red line) exhibited a bell-shaped irradiance profile, peaking at approximately 250 W/m² around solar noon (12-13 hours). The profiles showed a rapid increase in the morning, a stable peak and a gradual and equal reduction in the afternoon consistent with equatorial solar patterns. The calculated irradiance closely matches the PVGIS data throughout the day with the two curves overlapping significantly at the peak and during most of the daylight hours.

In Entebbe with a peak irradiance of 250 W/m² and a 10-hour daylight period, the model closely matched the PVGIS data reflecting the steady-state behaviour typical of equatorial climates.

5.1.2 Stockholm, Sweden (59.33°N, 18.06°E).

Stockholm represents a high-latitude northern location with big seasonal variation in solar availability. The long summer days and very short winter days, along with low solar elevation angles, make it a challenging environment. Validating the solar irradiation performance of the model in Stockholm tests its ability in low-radiation and high-variation environments.

For Stockholm, Sweden, the model is also evaluated on May 20th, with a tilt angle of 41° and an azimuth of -2°. The model's simulated global irradiance (W/m²) is compared against PVGIS reference data over a 24-hour solar time period.

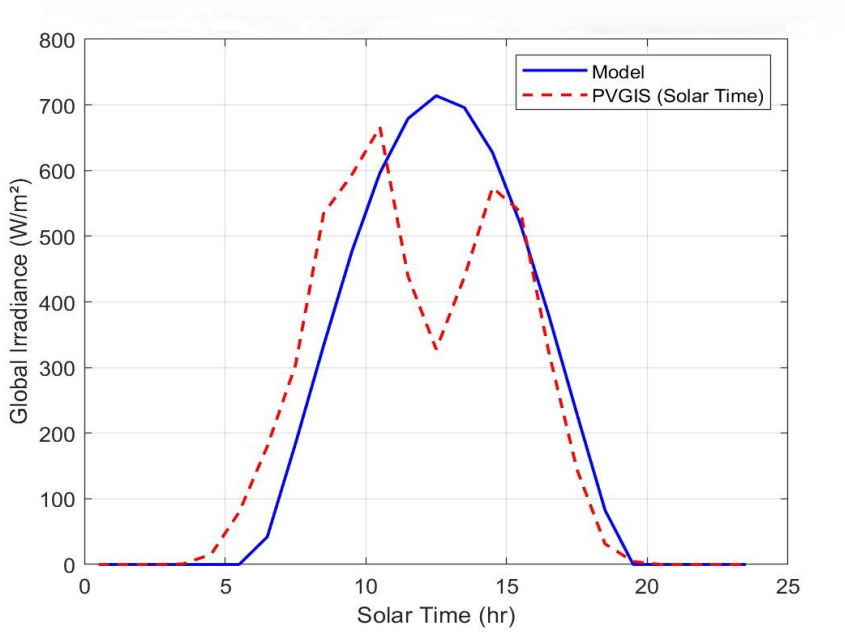


Figure 5-2 Comparison between analytical Model and calculated data (PVGIS) for Stockholm on 20th May

Both the model and PVGIS data showed a bell-shaped irradiance profile, peaking at 700 W/m² (model) and 650 W/m² (PVGIS) around solar noon (12-13hours). The irradiance increased significantly from 5hours and decreased after 18 hours, reflecting Stockholm's extended daylight hours in late spring.

The model generally followed the PVGIS data but missed the peak irradiance by approximately 50 W/m². The model's curve was smoother with a slower rise and fall compared to the sharper transitions in the PVGIS data, indicating less sensitivity to short-term variability.

The extended daylight and higher peak irradiance compared to equatorial regions (e.g., Entebbe) align with the expected solar patterns at Stockholm's latitude (59° N) during May, where the sun remains higher in the sky for longer periods.

In Stockholm, where the peak irradiance reached 700-750 W/m² over a 13hour daylight period, the model followed the overall profile but missed the peak by approximately 50 W/m² and smoothed out short-term variability.

5.1.3 Bloemfontein, South Africa (29.10°S, 26.20°E).

Bloemfontein, situated in the Southern Hemisphere, exhibits clear seasonal transitions between summer and winter. It receives relatively high levels of solar radiation, especially during summer. This location complements the other two cities by providing insight into performance in a southern mid-latitude setting with high radiation intensity.

For Bloemfontein, South Africa, with a tilt angle of 0° and an azimuth of 180°. The model's simulated global irradiance (W/m²) is also compared against PVGIS reference data over a 24hour solar time period.

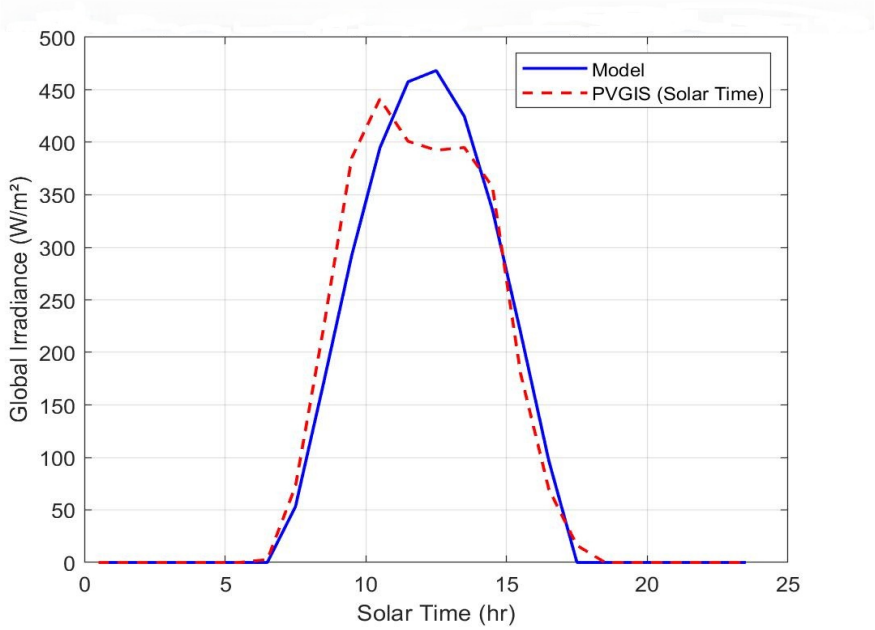


Figure 5-3 Comparison between analytical Model and calculated data (PVGIS) for Bloemfontein on 20th May

Both the model and PVGIS data exhibited a bell-shaped irradiance profile peaking at approximately 450 W/m² around solar noon (12-13hours). The irradiance increased significantly from 6 hours and decreased after 18 hours, reflecting a 12-hour period of significant solar input typical for a mid-latitude location in the Southern Hemisphere during late autumn. The model closely matched the PVGIS data with the two curves overlapping significantly at the peak and throughout most of the daylight hours.

The peak irradiance of 450 W/m² and the 12-hour daylight period align with expectations for Bloemfontein's latitude (29° S) in May where the sun is lower in the sky compared to summer months but still provides significant solar input due to the region's clear skies and elevation.

In Bloemfontein, with a peak of 450 W/m² over a 12-hour daylight period, the model aligned well with PVGIS data at the peak but exhibited a smoother curve, missing minor fluctuations observed in the reference data. This smoothing effect suggests that the model may rely on simplified assumptions such as clear-sky conditions or averaged atmospheric effects which do not fully account for real-world variability like cloud cover haze or diffuse radiation.

Finally, Comparing the three cities, the model performs best in Entebbe where climatic stability minimizes the impact of its limitations. Stockholm presents the greatest challenge with the model struggling to match the higher peak and variable conditions of a high-latitude spring. Bloemfontein falls between these extremes with the model performing well due to the region's relatively stable late-autumn conditions. These differences suggest that the model tends to be less accurate in areas with more complex atmospheric conditions something that could be useful to consider when improving it in the future.

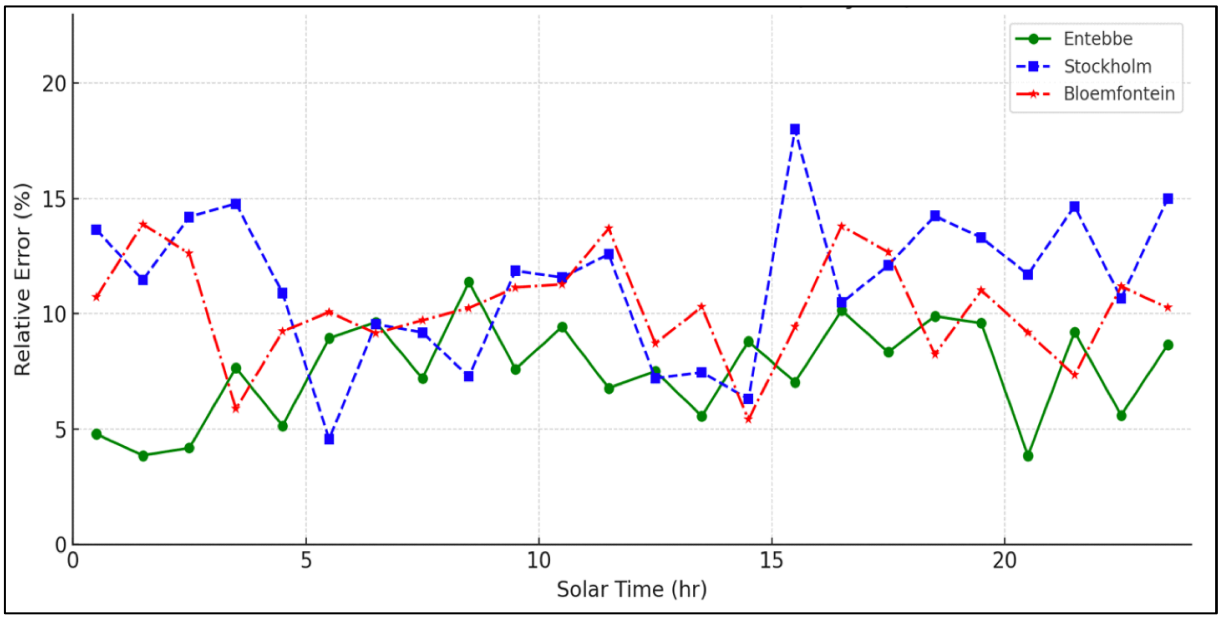


Figure 5-4 Relative Error of Model for the three cities on 20th May

The model shows the lowest relative error in Entebbe indicating good agreement with PVGIS data under stable equatorial conditions. Stockholm exhibits higher and more variable errors reflecting challenges in modelling at high latitudes with low solar angles. Bloemfontein shows moderate errors suggesting reasonable model accuracy in southern latitude conditions.

Below are discussions about the key results obtained from analysing the thermal performance of solar collectors across four cities Entebbe, Guardia, Bloemfontein and Stockholm as well as comparisons with photovoltaic (PV) systems. The aim was to understand how geography, particularly climate and latitude influences the performance of solar collectors.

5.1.4 Comparison of Solar Irradiance.

The comparison of the solar irradiance in four different cities Ghardaia, Stockholm, Entebbe and Bloemfontein serve as the basis for evaluating thermal solar collector and PV collector performance in the following sections. The solar irradiance trends were observed for typical days in January, July and October. (Table 3-3)

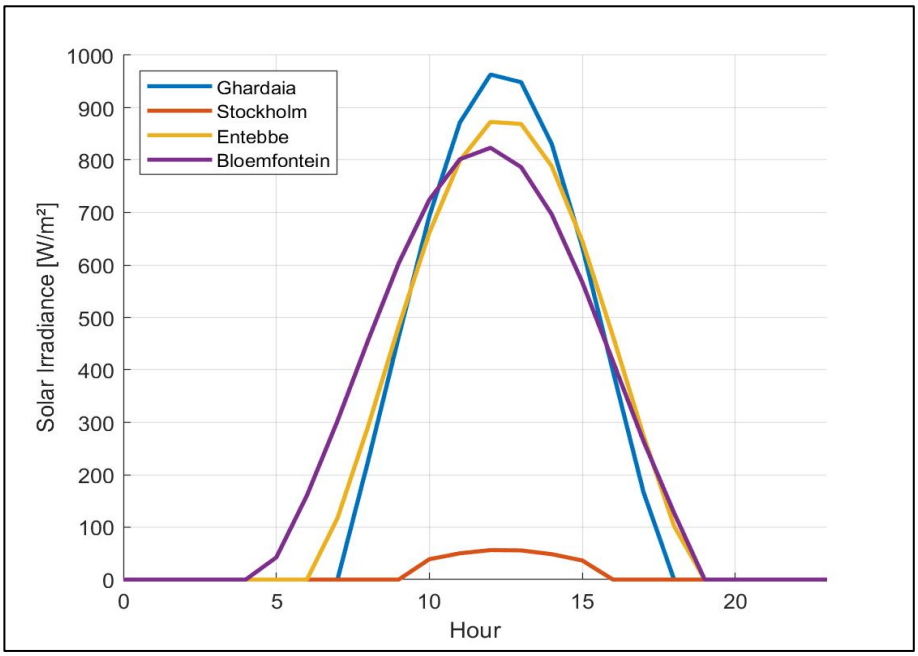


Figure 5-5: Solar Irradiance for January for all cities

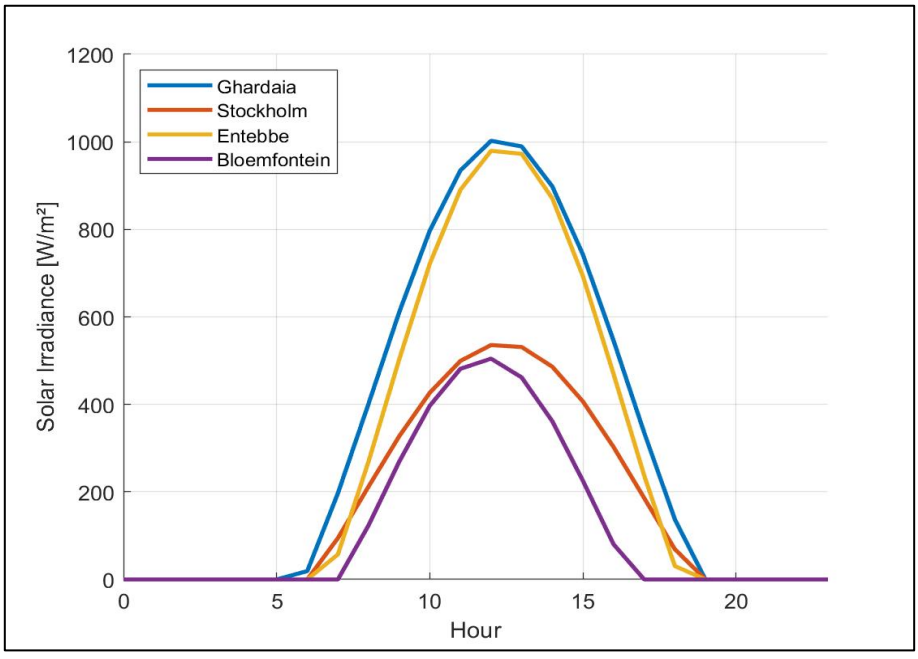


Figure 5-6: Solar Irradiance for July for all cities

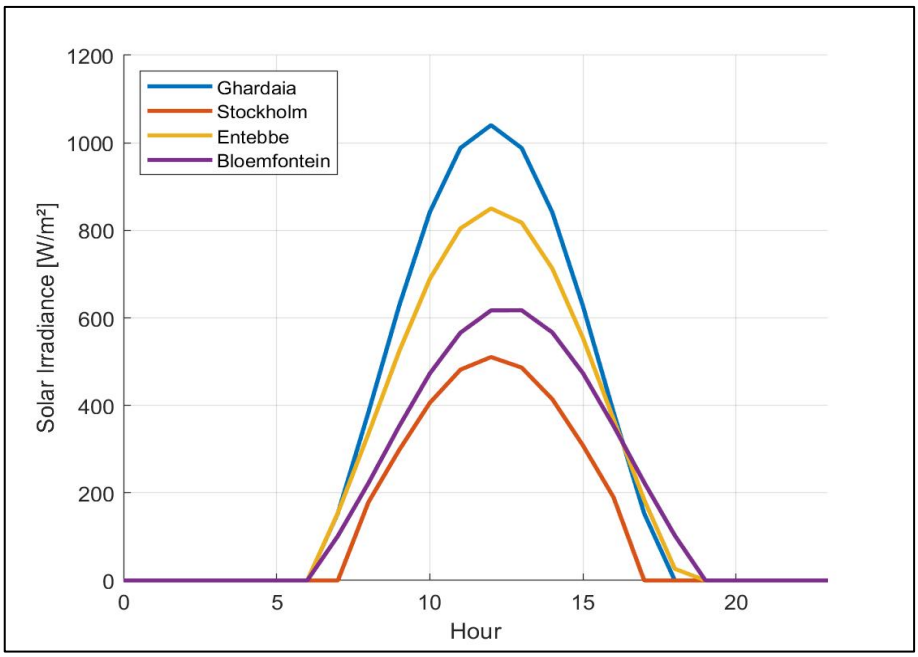


Figure 5-7: Solar Irradiance for October for all cities

The three Figures 5-5, Figure 5-6 and Figure 5-7 for January, July, and October illustrate the solar irradiation for the four cities Ghardaia located in the Sahara Desert records the highest irradiance levels throughout the year particularly in July. Bloemfontein also shows strong solar input especially during its summer month of January. Entebbe being near the equator displays a relatively stable irradiance profile across the selected months with only seasonal fluctuations in July. In contrast, Stockholm experiences significant seasonal variation with very low irradiance in January and higher levels in July and October.

This analysis confirms that local solar irradiance is a critical factor in determining the suitability and expected performance of solar collectors. It also emphasizes the need to tailor solar collector design and technology choices to the specific climatic conditions of each region.

5.1.5 Comparison of the Outlet Fluid Temperature.

Figures 5-8, 5-9 and 5-10 illustrate the comparisons of the outlet fluid temperature in the four different cities for January, July and October respectively.

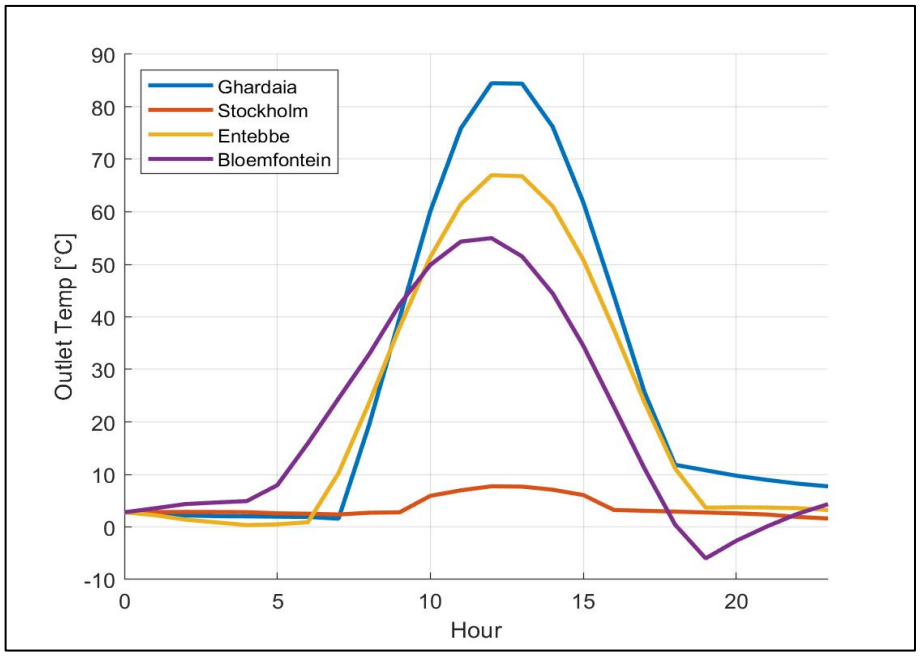


Figure 5-8: Outlet fluid temperature for January for all cities

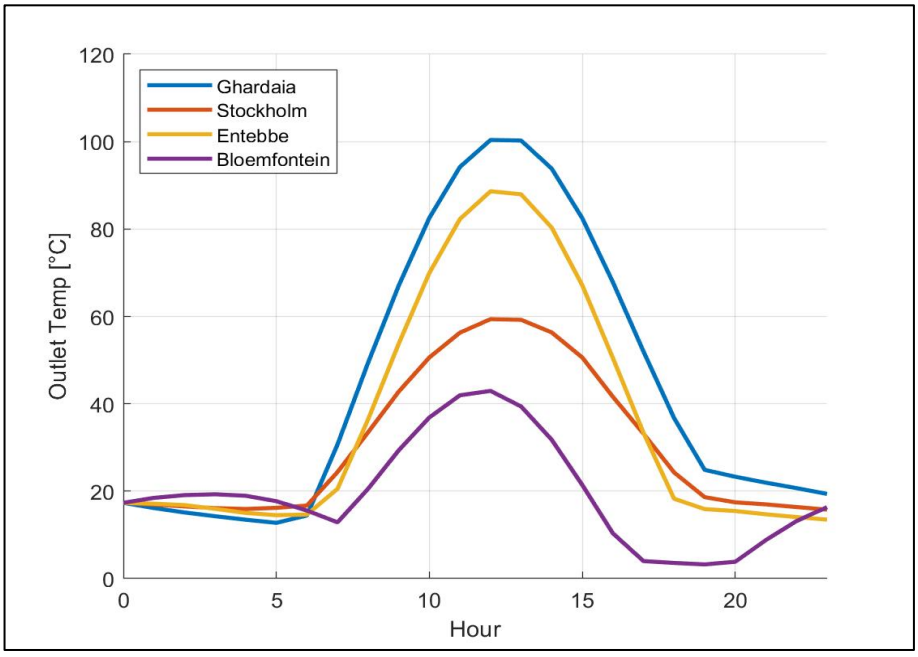


Figure 5-9: Outlet fluid Temperature for July for all cities

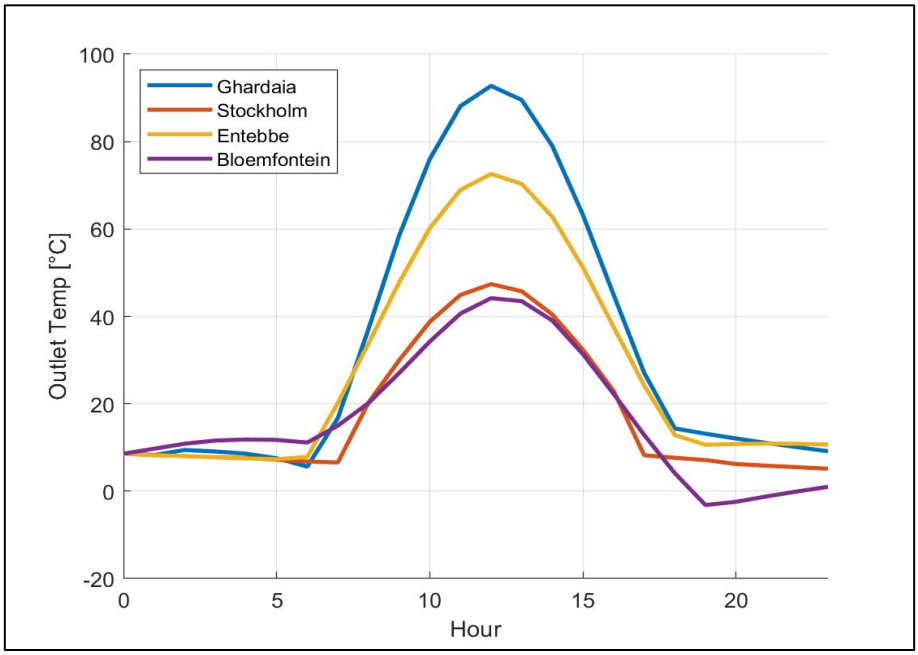


Figure 5-10: Outlet fluid Temperature for October for all cities

The outlet fluid temperatures for a typical day in January, July, and October shows clear variation across locations. Ghardaia has the highest outlet fluid temperatures in all three months especially in July when solar radiation levels are at their peak. Entebbe performs moderately well due to its consistent solar input throughout the year thanks to its equatorial location. Stockholm had the lowest temperatures particularly in January which is expected given its limited sunlight during winter.

These results highlight how flat plate collectors perform best in sunny and warm climates. Seasonal fluctuations in temperature were more noticeable in Ghardaia and Bloemfontein while Entebbe maintains relatively stable performance year-round. In contrast, Stockholm's low winter output emphasizes the challenge of using flat plate systems in high-latitude or cold regions without supplemental systems.

5.1.6 Comparison of the Thermal Power Output.

Figures 5-11, 5-12 and 5-13 illustrate comparisons of the thermal power output in the four different cities for January, July and October respectively.

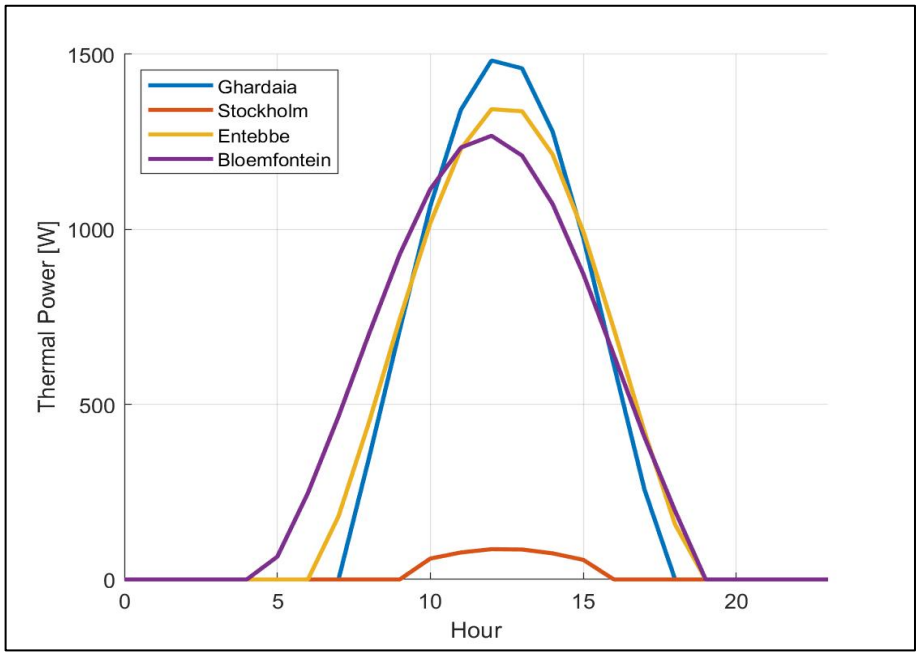


Figure 5-11 Thermal Power Output of January for all cities

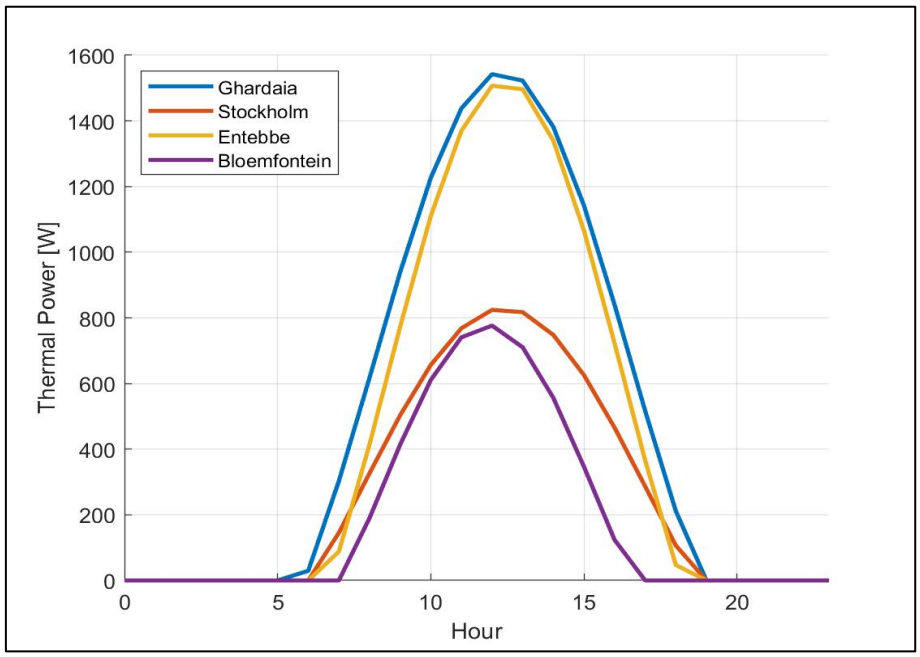


Figure 5-12 Thermal Power Output of July for all cities

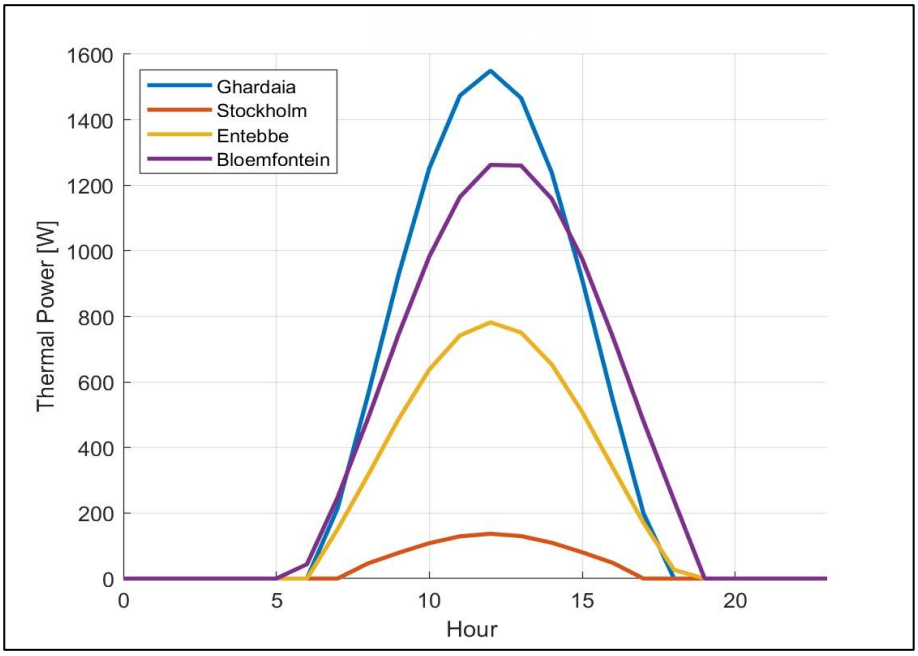


Figure 5-13 Thermal Power Output of October for all cities

The thermal power output of the solar collector varies significantly across the four cities Ghardaia, Entebbe, Bloemfontein and Stockholm when comparing the months of January, July and October.

In January, Ghardaia records the highest thermal power output due to its favourable desert climate and clear skies while Stockholm shows the lowest performance largely because of limited sunlight and low solar angles during the winter season. Entebbe situated near the equator maintains a relatively stable output across all three months reflecting minimal seasonal variation in solar radiation. Bloemfontein recorded the third highest power output because this is its summer month.

In July, thermal power output reaches its peak in most locations with Ghardaia and Entebbe showing particularly strong performance due to longer daylight hours and higher solar intensity. Stockholm also improves notably compared to January although its output remains lower than the other cities. Bloemfontein records the lowest power output because it is winter in July and hence the thermal power output is low due to low outlet fluid temperature.

By October, thermal power outputs begin to decline for most cities except Bloemfontein which increases. Overall, the results emphasise how solar thermal power performance is closely tied to both geographical location and season reinforcing the need for climate adapted Solar collectors and careful selection of their different collectors to match local conditions.

5.1.7 Solar Collector Efficiency

Figures 5-14 illustrates the solar collector efficiency of the four different cities Ghardaia, Stockholm, Entebbe and Bloemfontein respectively.

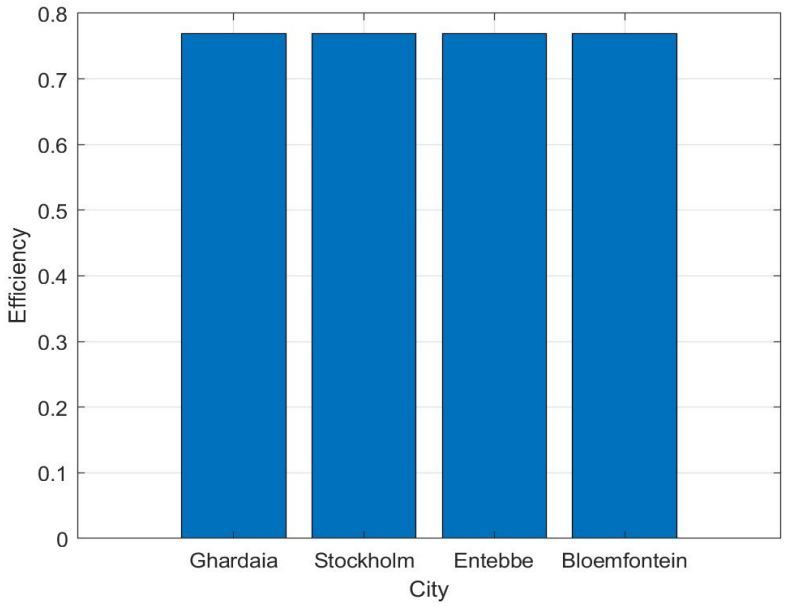


Figure 5-14 comparison of thermal collector efficiency by city

In the study, the thermal collector efficiency of the flat plate collector remained consistently high approximately 0.79 across all four cities (Entebbe, Guardia, Bloemfontein and Stockholm). This indicates that the collector efficiency depends on the device construction like geometrical and optical parameter and is not affected by diverse climatic conditions regardless of the season or geographic location.

5.1.8 Comparison between Average Monthly Thermal and PV power output for the months of January, July and October.

Figures 5-15, 5-16 and 5-17 illustrate the comparisons of the Solar Collector average monthly thermal and PV power output in the four different cities for the months of January, July and October.

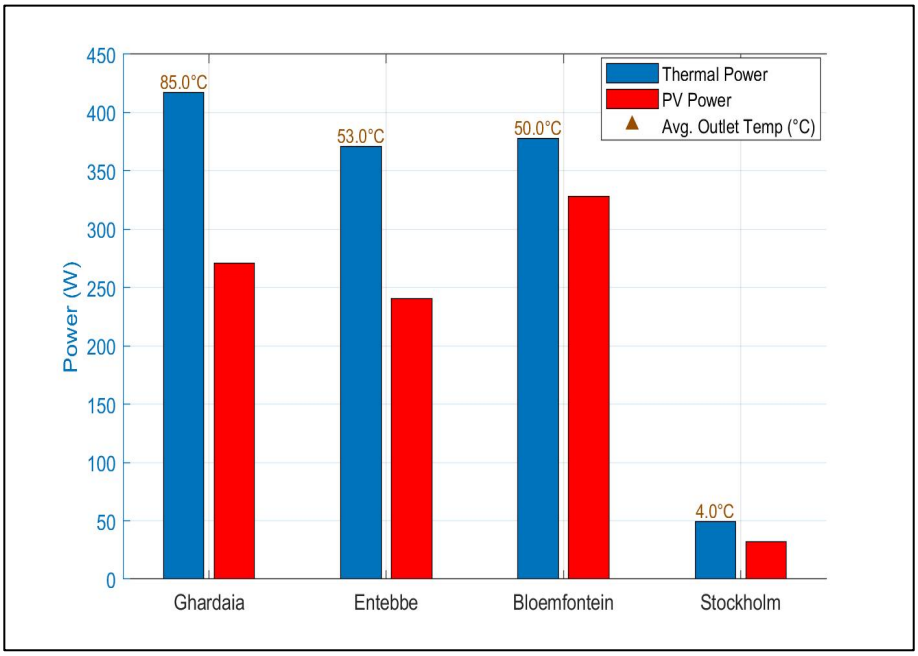


Figure 5-15 Thermal and PV Average Monthly Power Output of January for all cities

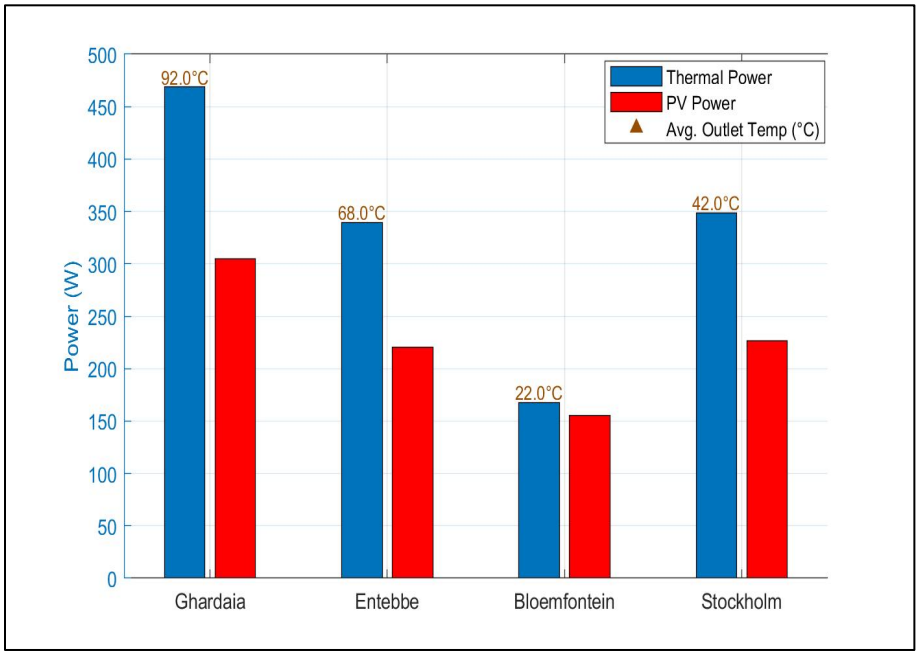


Figure 5-16 Thermal and PV Average Monthly Power Output of July for all cities

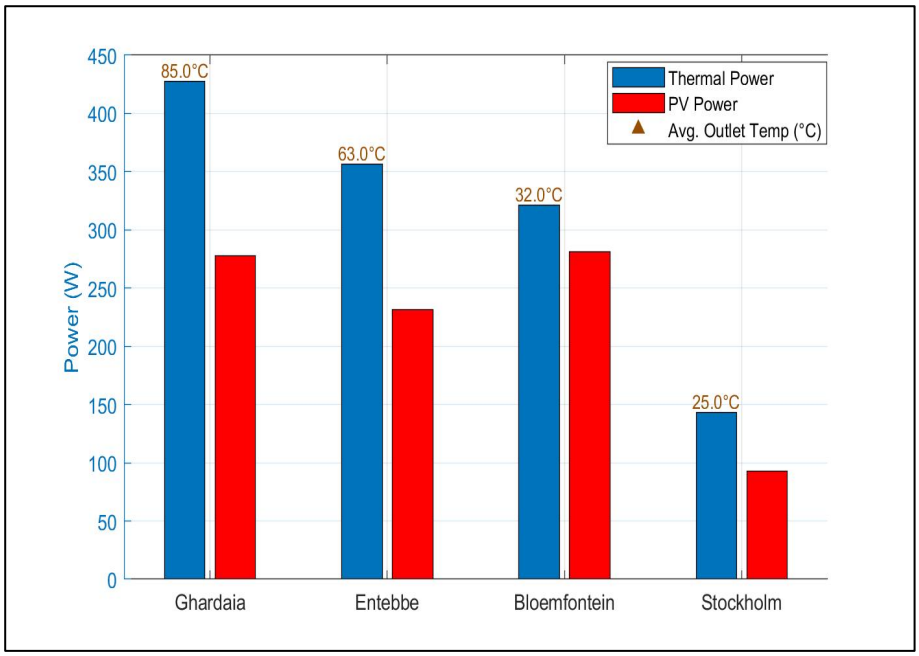


Figure 5-17 Thermal and PV Average Monthly Power Output of October for all cities

A comparison of average monthly power output between PV and thermal solar collectors for the months of January, July and October across Ghardaia, Entebbe, Bloemfontein and Stockholm reveal different performance trends influenced by climate and latitude. In Ghardaia and Entebbe, thermal collectors generally outperform PV due to high solar irradiance and favourable operating temperatures with minimal seasonal variation in Entebbe owing to its equatorial location.

In Bloemfontein, thermal collectors deliver higher output in its summer month of January while PV performance closely follows that of thermal collectors in its winter month of July due to its efficiency at lower temperatures. However, the outlet fluid temperature for the months of July and October is 22°c and 32°c which is low. Consequently, the thermal power output for these months is negligible and not competitive with PV.

Stockholm with its cold climate shows low outputs in January for both collectors, thermal collectors slightly outperform PV particularly in the summer month of July when long daylight hours and mild temperatures enhance thermal efficiency. However, the outlet fluid temperature for thermal collector for the months of January and October which is 4°c and 25°c is too low. Consequently, the thermal power output for these months is negligible and not competitive with PV.

5.1.9 Average Yearly Thermal Power Output of Solar Collectors.

Figure 5-18 illustrates the average yearly thermal power output of solar collectors.

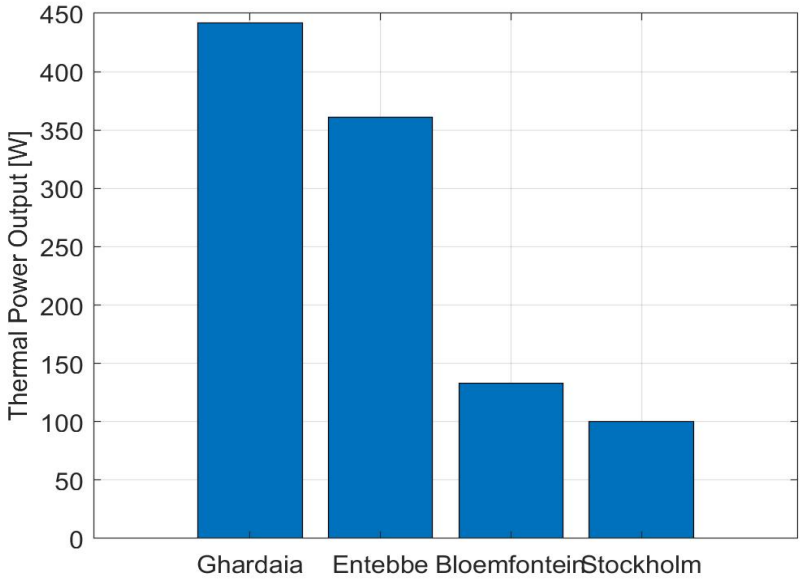


Figure 5-18: Average Yearly Thermal Power Output for all cities

Looking at the yearly average thermal power output, Ghardaia and Entebbe performs the best followed by Bloemfontein. Stockholm's performance is consistently the lowest.

This order reflects the influence of solar irradiance, ambient temperature and latitude on Solar collector performance. Ghardaia's desert climate offers high solar irradiance and hot conditions making it ideal for thermal energy generation.

Entebbe near the equator benefits from consistent solar exposure and warm temperatures though some cloud cover slightly reduces its output. Bloemfontein experiences moderate solar Output with seasonal variation and cooler winters while Stockholm's high latitude, low sun angles and cold climate significantly limit its thermal power potential.

These results indicate that the use of thermal solar system is insignificant in the areas above and below the latitude of 30° and -30° (Stockholm and Bloemfontein) respectively where PV is the optimal choice. They also align closely with the available solar resources in each city[36] and the results suggest that solar collectors in sunny climates can reliably produce significant amounts of energy year-round making them well-suited for domestic hot water industrial heating or agricultural activities in these regions.

5.1.10 Comparison between Average Yearly Thermal and PV power output.

Figure 5-19 illustrates the comparison between average yearly thermal and PV power output.

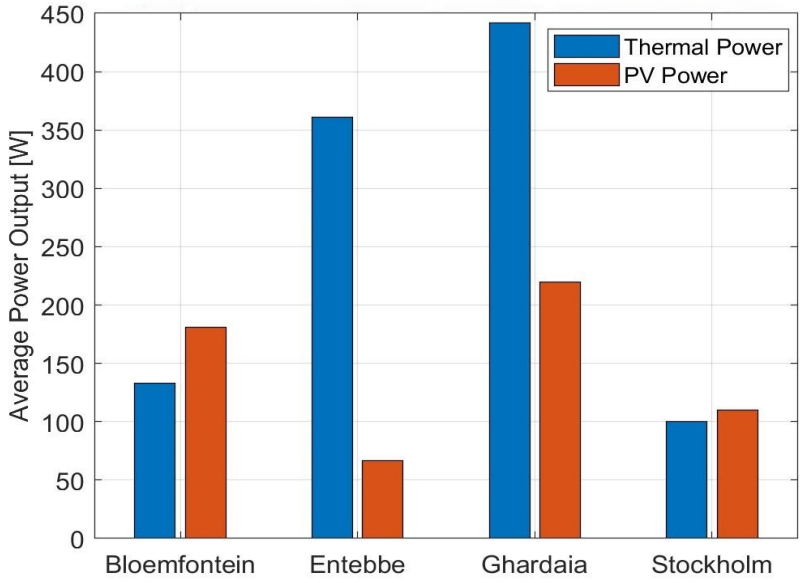


Figure 5-19: Comparison of Average Yearly Power Output for all 4 cities

Thermal collectors consistently deliver higher average power output in Ghardaia and Entebbe compared to PV collectors. For Bloemfontein and Stockholm, PV power slightly outperforms thermal power. Ghardaia records the highest values for both thermal collectors and PV collectors with thermal power output reaching approximately 445 W and PV output around 240W almost 50% of thermal power output reflecting the region's high solar irradiance and favourable climatic conditions.

Entebbe shows a relatively high thermal power output approximately 365W but a much lower PV power output approximately 70W which is 19% of thermal power likely due the fact that PV power output values are based on real climate values that is cloudy throughout the year.

Bloemfontein and Stockholm follow a different trend, with PV Power outperforming thermal power by considerably slight margin. This is because thermal solar collectors do not operate efficiently throughout the year but only in the summer season.

Overall, the comparison between the thermal and PV power indicate that the use of thermal solar system is insignificant in the areas above and below the latitude of 30° and -30° respectively where PV is the optimal choice.

General Conclusion.

This study analyses the performance of flat plate solar collectors through a structured five-chapter approach. Chapter 1 reviews prior research on solar collector systems. Chapter 2 explains the structural design and operational principles of flat plate collectors, showing the energy conversion mechanisms of each component. In Chapter 3, a mathematical model is developed based on solar parameter equations to estimate thermal performance incorporating solar radiation and heat losses. Chapter 4 describes the computational methodology using Matlab showing the algorithm used to analyse the collector's output. Finally, Chapter 5 presents analytical results across different geographic regions, validates the model and compares key performance metrics such as solar irradiance, thermal power output and outlet fluid temperature while linking findings to local climate conditions to assess the viability of solar thermal applications.

The thermal performance of solar collectors in four diverse locations; Entebbe, Ghardaia, Stockholm and Bloemfontein is analysed. Using hourly solar radiation models and assumes fixed inlet temperature. Performance modelling shows that solar energy availability varies significantly with location.

Ghardaia with high solar irradiance shows the strongest year-round performance. Entebbe near the equator has stable solar irradiance and consistent performance year-round. Bloemfontein and Stockholm have low thermal power output in their winter months but moderate gains in their summer months.

The results confirm that geographic and climatic conditions strongly affect solar collector output, emphasizing the need for site specific solar collector selection. This model-based approach provides a practical method for estimating solar collector performance where real data is limited.

Future studies should consider using hourly measured weather and solar irradiance data to better capture short-term variability, including measuring data of the inlet fluid temperature which would make the analytical model more accurate.

The only thermal system which is used in the study is a Flat plate solar collector. So, expanding the model to include concentrating collectors and Photovoltaic-Thermal hybrid systems could offer a broader perspective on solar technology performance across climates.

An economic dimension such as levelized cost of energy or return on investment, would further strengthen the study by connecting technical performance to financial feasibility.

References.

[1] ‘Hottel, H. and Woertz, B. (1942) Performance of Flat Plate Solar Heat Collectors. Transactions of the American Society of Mechanical Engineers, 64, 91-104. - References - Scientific Research Publishing’. Accessed: Jun. 05, 2025. [Online]. Available: https://www.scirp.org/reference/referencespapers?referenceid=1910447

[2] D. M. Medina Carril, J. G. Carrillo, R. D. Maldonado, and F. Avilés, ‘Finite element analysis of a solar collector plate using two plate geometries’, *Ing. E Investig.*, vol. 36, no. 3, pp. 95–101, Dec. 2016, doi: 10.15446/ing.investig.v36n3.56071.

[3] H. Tabor, ‘Use of solar energy for cooling purposes’, *Sol. Energy*, vol. 6, no. 4, pp. 136–142, Oct. 1962, doi: 10.1016/0038-092X(62)90124-X.

[4] K. M. Pandey and R. Chaurasiya, ‘A review on analysis and development of solar flat plate collector’, *Renew. Sustain. Energy Rev.*, vol. 67, pp. 641–650, Jan. 2017, doi: 10.1016/j.rser.2016.09.078.

[5] S. A. Kalogirou, *Solar Energy Engineering: Processes and Systems*. Elsevier, 2023.

[6] J. A. Duffie and W. A. Beckman, *Solar Engineering of Thermal Processes*. John Wiley & Sons, 2013.

[7] V. M Pandian, *Handbook of Research on Novel Soft Computing Intelligent Algorithms: Theory and Practical Applications: Theory and Practical Applications*. IGI Global, 2013.

[8] R. Awan, *Concentrated Solar Power Technologies*. Raafay Awan, 2021.

[9] J. Xia *et al.*, ‘Performance evaluation of different solar collectors in building cooling, heating, and hot water supply’, *J. Renew. Sustain. Energy*, vol. 12, no. 4, p. 043701, Jul. 2020, doi: 10.1063/1.5117268.

[10] ‘A Comparative Study on the Performances of Flat Plate and Evacuated Tube Collectors Deployable in Domestic Solar Water Heating Systems in Different Climate Areas’. Accessed: Apr. 13, 2025. [Online]. Available: https://www.mdpi.com/2225-1154/8/6/78

[11] ‘Comparison of the available solar radiation on flat-plate and concentrating solar collectors in Turkey · 研飞ivySCI’, 研飞ivySCI. Accessed: Apr. 13, 2025. [Online]. Available: https://www.ivysci.com/en/articles/4515073__Comparison_of_the_available_solar_radiation_on_flatplate_and_concentrating_solar_collectors_in_Turkey?utm_source=chatgpt.com

[12] ‘Techno-economic analysis of hybrid solar thermal systems with flat plate and parabolic trough collectors in industrial applications’, Ingeniería UC. Accessed: Apr. 14, 2025. [Online]. Available: https://www.ing.uc.cl/publicaciones/techno-economic-analysis-of-hybrid-solar-thermal-systems-with-flat-plate-and-parabolic-trough-collectors-in-industrial-applications/

[13] J. A. Duffie and W. A. Beckman, *Solar Engineering of Thermal Processes*. John Wiley & Sons, 2013.

[14] ‘Advanced Renewable Energy Sources - G. N. Tiwari, Rajeev Kumar Mishra - Google Books’. Accessed: Jun. 09, 2025. [Online]. Available: https://books.google.dz/books?hl=en&lr=&id=s8gng2vA_88C&oi=fnd&pg=PA483&dq=Tiwari,+G.+N.,+%26+Mishra,+R.+K.+(2012).+Advanced+Renewable+Energy+Sources.+Royal+Society+of+Chemistry.&ots=ucce98pjcj&sig=E1oAACqN9NZm4kIbcosn-OcE8xc&redir_esc=y#v=onepage&q=Tiwari%2C%20G.%20N.%2C%20%26%20Mishra%2C%20R.%20K.%20(2012).%20Advanced%20Renewable%20Energy%20Sources.%20Royal%20Society%20of%20Chemistry.&f=false

[15] S. A. Kalogirou, ‘Solar thermal collectors and applications’, *Prog. Energy Combust. Sci.*, vol. 30, no. 3, pp. 231–295, 2004, doi: 10.1016/j.pecs.2004.02.001.
[16] ‘A review of solar collectors and thermal energy storage in solar thermal’, ResearchGate. Accessed: Jun. 14, 2025. [Online]. Available: https://www.researchgate.net/publication/257157549_A_review_of_solar_collectors_and_thermal_energy_storage_in_solar_thermal
[17] ‘file_1731558700SHla9.pdf’. Accessed: Jun. 14, 2025. [Online]. Available: https://www.mechfamily-ju.com/storage/images/files/file_1731558700SHla9.pdf
[18] ‘principlesofsolarengi.pdf’. Accessed: Jun. 14, 2025. [Online]. Available: https://www.advan-kt.com/principlesofsolarengi.pdf
[19] Ž. Jesko, ‘Classification of solar collectors’.
[20] A. Ibrahim, M. Y. Othman, M. H. Ruslan, S. Mat, and K. Sopian, ‘Recent advances in flat plate photovoltaic/thermal (PV/T) solar collectors’, *Renew. Sustain. Energy Rev.*, vol. 15, no. 1, pp. 352–365, Jan. 2011, doi: 10.1016/j.rser.2010.09.024.
[21] Sunil. K. Amrutkar, ‘Solar Flat Plate Collector Analysis’, *IOSR J. Eng.*, vol. 02, no. 02, pp. 207–213, Feb. 2012, doi: 10.9790/3021-0202207213.
[22] J. Twidell and T. Weir, *Renewable Energy Resources*, 3rd ed. London: Routledge, 2015. doi: 10.4324/9781315766416.
[23] J. J. Michael, I. S, and R. Goic, ‘Flat plate solar photovoltaic–thermal (PV/T) systems: A reference guide’, *Renew. Sustain. Energy Rev.*, vol. 51, pp. 62–88, Nov. 2015, doi: 10.1016/j.rser.2015.06.022.
[24] A. Jamar, Z. A. A. Majid, W. H. Azmi, M. Norhafana, and A. A. Razak, ‘A review of water heating system for solar energy applications’, *Int. Commun. Heat Mass Transf.*, vol. 76, pp. 178–187, Aug. 2016, doi: 10.1016/j.icheatmasstransfer.2016.05.028.
[25] H. Bhowmik and R. Amin, ‘Efficiency improvement of flat plate solar collector using reflector’, *Energy Rep.*, vol. 3, pp. 119–123, Nov. 2017, doi: 10.1016/j.egyr.2017.08.002.
[26] K. M. Pandey and R. Chaurasiya, ‘A review on analysis and development of solar flat plate collector’, *Renew. Sustain. Energy Rev.*, vol. 67, no. C, pp. 641–650, 2017.
[27] H. Zondag, ‘Flat-plate PV-Thermal collectors and systems: A review’, *Renew. Sustain. Energy Rev.*, vol. 12, no. 4, pp. 891–959, May 2008, doi: 10.1016/j.rser.2005.12.012.
[28] J. M. Gordon, ‘Solar energy engineering: A mini-revolution in Israel’, *Refocus*, vol. 2, no. 2, pp. 34–37, Mar. 2001, doi: 10.1016/S1471-0846(01)80007-X.
[29] Y. Tian and C. Y. Zhao, ‘A review of solar collectors and thermal energy storage in solar thermal applications’, *Appl. Energy*, vol. 104, pp. 538–553, Apr. 2013, doi: 10.1016/j.apenergy.2012.11.051.
[30] R. Winston, ‘Principles of solar concentrators of a novel design’, *Sol. Energy*, vol. 16, pp. 89–95, Oct. 1974, doi: 10.1016/0038-092X(74)90004-8.
[31] A. M. Muzathik, M. Z. Ibrahim, K. B. Samo, and W. B. Wan Nik, ‘Estimation of global solar irradiation on horizontal and inclined surfaces based on the horizontal measurements’, *Energy*, vol. 36, no. 2, pp. 812–818, Feb. 2011, doi: 10.1016/j.energy.2010.12.035.
[32] M. Collares-Pereira and A. Rabl, ‘The average distribution of solar radiation-correlations between diffuse and hemispherical and between daily and hourly insolation values’, *Sol. Energy*, vol. 22, no. 2, pp. 155–164, Jan. 1979, doi: 10.1016/0038-092X(79)90100-2.
[33] M. Paulescu *et al.*, ‘Ångström–Prescott equation: Physical basis, empirical models and sensitivity analysis’, *Renew. Sustain. Energy Rev.*, vol. 62, pp. 495–506, Sep. 2016, doi: 10.1016/j.rser.2016.04.012.

[34] B. Y. H. Liu and R. C. Jordan, ‘The interrelationship and characteristic distribution of direct, diffuse and total solar radiation’, *Sol. Energy*, vol. 4, no. 3, pp. 1–19, Jul. 1960, doi: 10.1016/0038-092X(60)90062-1.
[35] ‘pvgis.com - PVGIS 5.3 SOLAR PANEL CALCULATOR’. Accessed: Jun. 15, 2025. [Online]. Available: https://pvgis.com/en/pvgis-5-3
[36] ‘JRC Photovoltaic Geographical Information System (PVGIS) - European Commission’. Accessed: Jun. 15, 2025. [Online]. Available: https://re.jrc.ec.europa.eu/pvg_tools/en/#MR